Physica D 485 (2026) 135031

Contents lists available at ScienceDirect

Physica D

journal homepage: www.elsevier.com/locate/physd

Breakdown of homoclinic orbits to L_1 of the hydrogen atom in a circularly polarized microwave field

Amadeu Delshams [a,b], Mercè Ollé [c,b,d], Juan Ramon Pacha [c], Óscar Rodríguez [c,b,*]

[a] Lab of Geometry and Dynamical Systems, Universitat Politècnica de Catalunya (UPC), Barcelona, Spain
[b] IMTech, Universitat Politècnica de Catalunya (UPC), Barcelona, Spain
[c] Department of Mathematics, Universitat Politècnica de Catalunya (UPC), Barcelona, Spain
[d] Centre de Recerca Matemàtica, Barcelona, Spain

ARTICLE INFO

Communicated by Alessandra Celletti

Keywords:
Hamiltonian dynamics
Exponentially small phenomena
Melnikov method
Multiple precision computations

ABSTRACT

We consider the Rydberg electron in a circularly polarized microwave field, whose dynamics is described by a 2 d.o.f. Hamiltonian, which is a perturbation of size $K > 0$ of the standard rotating Kepler problem. In a rotating frame, the largest chaotic region of this system lies around a saddle–center equilibrium point L_1 and its associated invariant manifolds. We compute the distance between stable and unstable manifolds of L_1 by means of a semi-analytical method, which consists of combining normal form, Melnikov, and averaging methods with numerical methods performed with multiple precision computations. Also, we introduce a new family of Hamiltonians, which we call *Toy CP systems*, to be able to compare our numerical results with the existing theoretical results in the literature. It should be noted that the distance between these stable and unstable manifolds is exponentially small in the perturbation parameter K (in analogy with the L_3 libration point of the R3BP).

1. Introduction

1.1. State of the art of the CP problem

The *CP Problem* consists of the motion in an hydrogen atom placed in an external circularly polarized microwave field. This system has been intensively studied, both experimentally [1–3], as theoretically, from classical [4–8] and quantum [6,9,10] points of view, as well as numerically [11–18]. In a rotating frame (see Section 1.2), the CP problem reads as a 2 degree-of-freedom (d.o.f.) Hamiltonian system. For a small enough field strength or a large enough angular frequency of the microwave field, the CP problem turns out to be just a perturbation of some size, say $K > 0$, of the rotating Kepler problem, and by KAM theory (see, for instance, [19, p. 276]) the phase space is full of 2-dimensional invariant tori with non-commensurable frequencies, except for the resonant zones around commensurable frequencies, which fill a domain of relative size $\mathcal{O}\left(\sqrt{K}\right)$. These 2-dimensional KAM tori preclude the existence of unstable trajectories, and in particular of *ionization*, that is, the loss of the electron, which turns out to be the main topic dealt with in all these studies. Consequently, ionization only takes place when all KAM invariant tori break, which happens when the perturbation parameter K is not so small.

However, for small K, the motion is not completely regular, and erratic trajectories can appear. Such kind of chaotic motion takes place outside the KAM tori, and is typically associated with the existence of saddle invariant objects. There are, at least, three zones where saddle objects may appear in the CP problem: (i) near collision with the nucleus, inside the first KAM torus, (ii) very far of the nucleus, say at infinity, outside the last KAM torus, and (iii) in the resonant zones, between the KAM invariant tori.

The aim of this work is to study the largest chaotic resonance zone, which happens to be associated with the lowest-order commensurability of the frequencies of the unperturbed invariant tori, and takes place around a saddle–center equilibrium point in a rotating frame, called L_1, together with its associated invariant unstable and stable manifolds. Saddle Lyapunov periodic orbits emerge from L_1, which are very important, indeed crucial, for the global behavior of the system [16]. As a matter of fact, it is a standard principle in dynamical systems that the saddle-invariant objects and their associated invariant manifolds are the main landmarks for understanding the global dynamical behavior of a dynamical system.

* Corresponding author.
E-mail addresses: Amadeu.Delshams@upc.edu (A. Delshams), Merce.Olle@upc.edu (M. Ollé), Juan.Ramon.Pacha@upc.edu (J.R. Pacha), oscar.rodriguez@upc.edu (Ó. Rodríguez).

https://doi.org/10.1016/j.physd.2025.135031
Received 8 June 2025; Received in revised form 7 November 2025; Accepted 8 November 2025
Available online 17 November 2025

Using an adequate cross-section, we measure the distance between the two branches of unstable and stable asymptotic trajectories to L_1, which turns out to be positive and exponentially small with respect to the perturbation parameter K. This is a consequence of the fact that L_1 is a *weak* saddle–center equilibrium point, that is, with saddle–center characteristic exponents $\pm\Lambda$, $\pm i\Omega$ for positive Λ, Ω, but with a *saddle–center ratio* $\Lambda/\Omega = \mathcal{O}\left(\sqrt{K}\right)$ tending to zero when the size of the perturbation K tends to zero.

The asymptotic formula found for this distance d takes the form

$$d \sim \varepsilon^j A\,|\omega|^r \exp(b\,\omega), \text{ with } \omega = -\frac{1}{3\varepsilon^2} \text{ and } \varepsilon = \left(\frac{K}{3}\right)^{1/4},$$

where j will depend on the model considered (besides the CP problem we will analyze other problems as well), b, r and A are the constants to be fitted, ordered in increasing order of numerical difficulty: first b is fitted, then r and finally the constant A, which is the one that poses the most difficulty, and for which we have not always been able to provide a significant number of decimals. One of the main reasons is that the perturbation parameter K appears in the above asymptotic formula raised to an exponent $1/2$ or $1/4$, and so it is necessary to consider K extraordinarily small in order to provide a good asymptotic approximation. A summary of results is provided in Section 6.

The measurement of this distance has been mostly carried out numerically (6)–(7), although in some cases it has been possible to verify it with theoretical formulas (32) with a fairly good agreement, although its exponential smallness makes a very precise fitting difficult.

The numerical measure requires dealing with high-precision computations (using up to five thousand digits) combined with the parameterization method –using an order of (up to) one thousand in the expansions involved– (described in Appendix B) to get a local computation of the invariant manifolds, as well as Taylor method (implemented on a robust, fast, and accurate package by Jorba and Zou [20]) to integrate the system without a significant loss of precision. Multiple precision calculations have been performed using the `mpfr` library (see [21]).

Analytic approximations are also obtained for the invariant manifolds of L_1. For this, we simply introduce action–angle variables, which are nothing more than the Delaunay variables for the Kepler problem, combined with a subsequent change to the Poincaré variables to avoid the degeneracy of the circular solutions of Kepler's problem. In these variables, the CP problem consists of a perturbation of an integrable system formed by an isochronous rotor plus an *amended* pendulum. This *amended* pendulum depends on the perturbation parameter and gives rise to two *separatrices*, which also depend on the perturbation parameter.

When the perturbation is taken into account, we introduce a direct approximation of the splitting of these separatrices, based on the study of the variational equations along them (this is the so-called Melnikov method) and we compare the distance between these approximate invariant manifolds with the one obtained with the aforementioned numerical calculations, performed both in synodic coordinates (6) for the rotating frame (in the Poincaré section $y = 0$), and in Poincaré variables (7).

We have also verified that, to have a good analytical approximation, it is crucial to choose the right amended pendulum. For this reason, we also present an additional approximation equivalent to the Melnikov method, based on the application of the averaging method. We check that the choice of an adequate degree of the amended pendulum as a function of the perturbation parameter is totally necessary to obtain a good fit with the numerical calculations.

Unfortunately, there are no general theoretical results in the literature that can be directly applied to prove analytically the numerical results found for the CP problem, due to the fact that the perturbation presents a high-order singularity and that the integrable Hamiltonian where perturbative theoretical methods should be applied depends essentially on the perturbative parameter K. To discuss whether Melnikov method, when applied to a Hamiltonian given by an integrable part plus a perturbation, correctly predicts the found fitting formulas, it is necessary to consider both the integrable part and the perturbation.

This discussion has led us to the analysis of a more general Hamiltonian that we have called *Toy CP problem* (9), which, apart from K, also depends on two other parameters a and m. More details are provided in Section 1.4. The observed phenomenology opens the door to a new world of theoretical studies.

It has to be noticed that the distance studied is much smaller in one of the separatrix, the *internal* one, than in the other one, the *external* separatrix. For this reason, in this paper we focus on measuring the distance between the external asymptotic trajectories to L_1.

This is a first step to measuring the distance between the two branches of asymptotic unstable and stable surfaces to the Lyapunov periodic orbits close to L_1, and to show that they intersect along only two transverse homoclinic orbits. This computation will be performed in a future paper, and will provide a measure of the chaotic region close to L_1, which is proportional to the transversality of these branches.

It is worth remarking that the CP problem is similar to the Planar Circular Restricted 3-Body Problem (R3BP), since both are perturbations of the rotational Kepler problem. Since the equilibrium point L_1 of the CP problem is a weak saddle–center, it is also similar to the libration point L_3 of the R3BP, where similar features happen and theoretical results are available [22,23]. Therefore, we have applied a number of tools coming from Celestial Mechanics or, more generically, Hamiltonian systems, like invariant manifolds, Melnikov method, averaging method, etc.

1.2. The model for the CP problem

In the simplest case (assuming *planar* motion for the electron) the *classical* motion is governed by a system of two 2nd-order ODE

$$\ddot{X} = -\frac{X}{R^3} - F\cos(\varpi s), \qquad R^2 = X^2 + Y^2,$$
$$\ddot{Y} = -\frac{Y}{R^3} - F\sin(\varpi s), \qquad \dot{} = \frac{\mathrm{d}}{\mathrm{d}s},$$

where $\varpi > 0$ is the *angular frequency of the microwave field* and $F > 0$ is the *field strength*.

This system can be written as a periodic in time 2 d.o.f. Hamiltonian

$$H(X, Y, P_X, P_Y) = \frac{1}{2}\left(P_X^2 + P_Y^2\right) - \frac{1}{R} + F\left(X\cos(\varpi s) + Y\sin(\varpi s)\right).$$

As in the R3BP (Restricted 3-Body Problem), we can get rid of the time dependence introducing rotating coordinates $\left(\widetilde{X}, \widetilde{Y}, P_{\widetilde{X}}, P_{\widetilde{Y}}, s\right)$

$$\begin{pmatrix}\widetilde{X}\\ \widetilde{Y}\end{pmatrix} = R(\varpi s)\begin{pmatrix}X\\ Y\end{pmatrix}, \quad \begin{pmatrix}P_{\widetilde{X}}\\ P_{\widetilde{Y}}\end{pmatrix} = R(\varpi s)\begin{pmatrix}P_X\\ P_Y\end{pmatrix}, \quad R(\varpi s) = \begin{pmatrix}\cos\varpi s & \sin\varpi s\\ -\sin\varpi s & \cos\varpi s\end{pmatrix}$$

to get an *autonomous* Hamiltonian

$$H\left(\widetilde{X},\widetilde{Y},P_{\widetilde{X}},P_{\widetilde{Y}}\right)=\frac{1}{2}\left(P_{\widetilde{X}}^2+P_{\widetilde{Y}}^2\right)-\frac{1}{\widetilde{R}}-\varpi\left(\widetilde{X}P_{\widetilde{Y}}-\widetilde{Y}P_{\widetilde{X}}\right)+F\widetilde{X},$$

where $\widetilde{R}^2=\widetilde{X}^2+\widetilde{Y}^2$. To get rid of the angular frequency ϖ we perform the change $(\widetilde{X},\widetilde{Y})=a(x,y)$, $\left(P_{\widetilde{X}},P_{\widetilde{Y}}\right)=a\varpi(p_x,p_y)$, which is a symplectic transformation with multiplier $a^2\varpi$ with $a=1/\varpi^{2/3}$, plus a scaling in time $\tilde{s}=\varpi s$ to get a new Hamiltonian in the rotating and scaled coordinates (x,y,p_x,p_y), usually also called synodic coordinates in the literature.

$$\mathcal{H}(x,y,p_x,p_y)=\frac{1}{2}(p_x^2+p_y^2)-\frac{1}{r}-(xp_y-yp_x)+Kx,\qquad r=\sqrt{x^2+y^2},\tag{1}$$

where $K=F/\varpi^{4/3}>0$, with associated Hamiltonian equations

$$\begin{aligned}\dot{x}&=p_x+y,\quad &\dot{p}_x&=p_y-\frac{x}{r^3}-K,\\ \dot{y}&=p_y-x,\quad &\dot{p}_y&=-p_x-\frac{y}{r^3},\end{aligned}\tag{2}$$

being now $\dot{}=d/d\tilde{s}$. It is very important and useful to realize that this Hamiltonian system is invariant under the reversibility

$$(\tilde{s},x,y,p_x,p_y)\mapsto(-\tilde{s},x,-y,-p_x,p_y).\tag{3}$$

Note that for the case $K=0$ the system reduces to the *rotating Kepler Hamiltonian*. While the parameter K appears solely in an additive form within the equation for the momentum p_x in Eqs. (2), the situation changes significantly when $K>0$, and the dynamic of the CP problem become much more complicated than the one of the rotating Kepler problem. See for example [16], where the behavior of the CP problem is shown to exhibit erratic motion before ionization, with hyperbolic periodic orbits playing a key role, or [18] where the dynamics associated with the families of ejection-collision orbits and their bifurcations are studied.

In the literature, it is also typical to find the system associated with the Hamiltonian (1) written as a system of second-order ODE

$$\begin{aligned}\ddot{x}-2\dot{y}&=\Omega_x(x,y),\\ \ddot{y}+2\dot{x}&=\Omega_y(x,y),\end{aligned}\tag{4}$$

where

$$\Omega(x,y)=\frac{1}{2}r^2+\frac{1}{r}-Kx,$$

and $r=\sqrt{x^2+y^2}$. In this way, the system (4) has a first integral, known as the Jacobi first integral, defined by

$$C=2\Omega(x,y)-(\dot{x}^2+\dot{y}^2),\tag{5}$$

and related to the Hamiltonian (1) by $C=-2\mathcal{H}$. For a fixed value of K and the first integral C, the admissible regions of motion, known as Hill regions, are defined by

$$\mathcal{R}=\mathcal{R}(K,C)=\left\{(x,y)\in\mathbb{R}^2\mid 2\Omega(x,y)\geq C\right\}.$$

1.3. Invariant objects

The equations for equilibrium points $\dot{x}=\dot{y}=\dot{p_x}=\dot{p_y}=0$ in system (2) are just

$$p_x=-y,\qquad p_y=x,\qquad x-\frac{x}{r^3}=K,\qquad y-\frac{y}{r^3}=0,$$

which give a whole circle $r=1$ for $K=0$, that is, for the rotating Kepler Hamiltonian. For the CP problem $K>0$ there are just two equilibrium points

$$L_1=(x_1,0,0,x_1),\qquad L_2=(x_2,0,0,x_2),$$

with $x_1^3-Kx_1^2+1=0$ and $x_2^3-Kx_2^2-1=0$ so that $x_1=x_1(K)$, $x_2=x_2(K)$ are of the form

$$x_1(K)=-1+\frac{K}{3}+\mathcal{O}\left(K^2\right),\qquad x_2(K)=-x_1(-K)=1+\frac{K}{3}+\mathcal{O}\left(K^2\right).$$

Since L_i are critical points of the potential, the topology of the Hill regions changes at the values of the Jacobi constant corresponding to these points, or equivalently, at the values $h_i=\mathcal{H}(L_i)$ of the Hamiltonian (1), for $i=1,2$.

Note that for values $\mathcal{H}\leq h_1$, ionization cannot occur, and for values $\mathcal{H}\geq h_2$, the entire configuration space becomes a valid region of motion (see Fig. 1). This is of significant importance, as the point L_1 and the dynamics associated with the invariant objects emanating from it act as the channel for ionization at the lowest energy levels where it is possible.

In particular, L_1 is a saddle–center equilibrium point for all $K>0$, with characteristic exponents $\pm\Lambda$, $\pm\mathrm{i}\Omega$ with

$$\Lambda=\sqrt{3K}(1+\mathcal{O}(K)),\quad \Omega=1+\mathcal{O}(K),$$

and associated 1D invariant manifolds, $W^{\mathrm{u}}(L_1),W^{\mathrm{s}}(L_1)$, which live in the energy level $\mathcal{H}=h_1=\mathcal{H}(L_1)$. Emerging form L_1 there is a family of saddle Lyapunov periodic orbits OL around L_1 for $h>h_1$, with associated 2D-invariant manifolds $W^{\mathrm{u}}(OL),W^{\mathrm{s}}(OL)$, also called *whiskers*.

Notice that the saddle character of L_1 is *weak* with respect to the parameter K, because its *saddle–center ratio* $\Lambda/\Omega=\sqrt{3K}(1+\mathcal{O}(K))$ tends to 0 as K tends to 0. This will imply a very small distance between $W^{\mathrm{u}}(L_1)$ and $W^{\mathrm{s}}(L_1)$ and a very small transversality between $W^{\mathrm{u}}(OL)$ and $W^{\mathrm{s}}(OL)$, indeed exponentially small in K. This weak saddle–center character of L_1 is totally analogous to the weak saddle–center character of the libration point L_3 of the R3BP (see [22]).

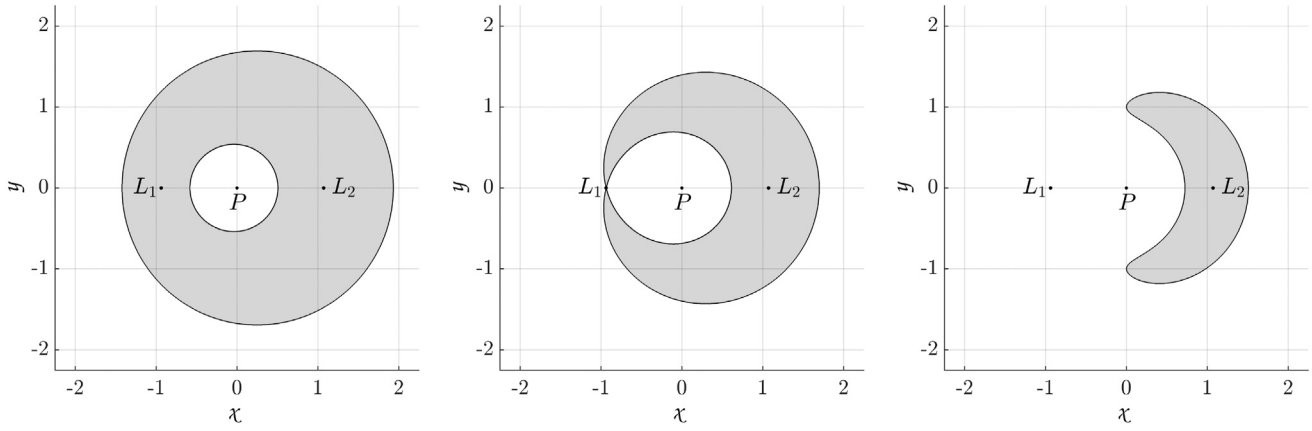

Fig. 1. In gray the forbidden region of motion for $K = 0.2$ and $\mathcal{H} = -2 < h_1$, $\mathcal{H} = h_1$ and $\mathcal{H} = -1.5 \in (h_1, h_2)$ from left to right. P denotes the position of the nucleus.

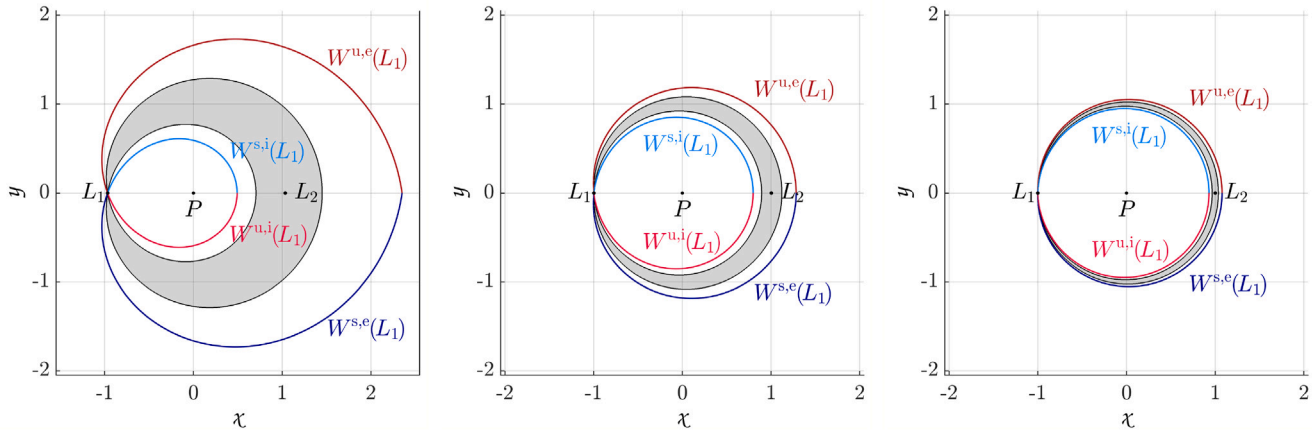

Fig. 2. (x, y) projection of the external $W^{u,e}(L_1)$ and internal $W^{u,i}(L_1)$ unstable manifolds of L_1 (similarly for the stable ones) for $K = 0.1$, 0.01 and 0.001 from left to right. In gray the forbidden region of motion for h_1.

In this paper, we will focus only on the invariant manifolds $W^u(L_1), W^s(L_1)$. We distinguish between the external branches of the manifolds, $W^{u,e}(L_1)$, $W^{s,e}(L_1)$ and the internal branches $W^{u,i}(L_1)$, $W^{s,i}(L_1)$. The four different branches for $K = 0.1$, 0.01 and 0.001 are displayed in Fig. 2. Notice that the external branches seem to coincide (similarly the internal ones) but they do not. Precisely, the purpose of this paper is to analyze the small distance — splitting — between them.

Actually we will concentrate on the external branches that will be simply denoted, from now on, by $W^u(L_1), W^s(L_1)$ (unless there are possible misunderstandings).

1.4. Main results

We enumerate the main results obtained and provide the location and quotation to equations (along the paper) where they are analyzed.

1. For the CP problem (1) we have numerically found an asymptotic formula for the splitting between the invariant unstable and stable manifolds (external branches) of L_1, $W^{u,s}(L_1)$, at (the first crossing with) $y = 0$ in synodic (rotating) coordinates $(x, y, \dot{x}, \dot{y})$ (2), which has the expression

$$\Delta\dot{x} \sim \varepsilon A|\omega|^r \exp\left(\frac{\omega\pi}{2}\right), \qquad \varepsilon = \left(\frac{K}{3}\right)^{1/4}, \quad \omega = -\frac{1}{3\varepsilon^2} = -\frac{1}{\sqrt{3K}}, \tag{6}$$

with $r = r_{CP} = 1.61111\ldots = 29/18$ and the leading constant $A = A_{CP} = 16.055307843\ldots$ See (44) and (48) in Section 3.2.

2. We obtain a similar asymptotic formula for the same splitting but computed in Poincaré (or *resonant*) variables (x, y, q, p), (11) and (14),

$$|\Delta p| \sim \varepsilon A|\omega|^r \exp\left(\frac{\omega\pi}{2}\right), \tag{7}$$

see (49), with $r = r_{CPR} = 2.11111\ldots = 19/9 = r_{CP} + 1/2$ and the leading constant $A = A_{CPR} = 27.80860891\ldots$ (see (52) in Section 3.3), where the addition of $1/2$ to r_{CP} to get r_{CPR} and the relation between A_{CP} and A_{CPR} are well justified due to the non-canonical change from synodic to resonant variables (11). See (56) in Section 3.3.

3. We emphasize the "key point" of the resonant variables: the analysis of the behavior of the invariant manifolds $W^{u,s}(L_1)$ for the CP problem can be regarded as the behavior of a perturbation of a homoclinic separatrix. Indeed, the Hamiltonian in the resonant variables (11), (14) is

$$H_{\text{CPR}}(x,y,q,p)=\omega\frac{q^2+p^2}{2}+\frac{y^2}{2}+\cos x-1+\varepsilon H_1(x,y,q,p;\varepsilon),$$

and the homoclinic separatrix is given by $q=p=0$ and (21).

4. We show numerically that the Melnikov method predicts correctly the numerical asymptotic results (7), as long as we take a *suitable* integrable Hamiltonian system, formed by a rotor and an *amended* pendulum, which is not the standard pendulum of the case $\varepsilon=0$ (as is also the case in many other problems, see, for instance, [24–27]). To do so, we consider a *truncated* Hamiltonian once we have applied a change of variables (from synodic to Poincaré ones). More precisely,

$$H_{1,1}(x,y,q,p)=\omega\frac{q^2+p^2}{2}+\frac{y^2}{2}+\cos x-1-\frac{2}{3}\varepsilon^2y^3+\varepsilon\left(\frac{3q}{2}-\frac{q}{2}\cos 2x-\frac{p}{2}\sin 2x\right),\ \omega=\frac{1}{3\varepsilon^2}. \tag{8}$$

5. We introduce a new family of perturbations of a fast rotor and a pendulum, that we call *Toy CP problem*

$$H_{a,m}(x,y,q,p)=\omega\frac{q^2+p^2}{2}+\frac{y^2}{2}+\cos x-1-\frac{2a}{3}\varepsilon^2y^3+\varepsilon^m\left(\frac{3q}{2}-\frac{q}{2}\cos 2x-\frac{p}{2}\sin 2x\right) \tag{9}$$

with $\omega=\frac{1}{3\varepsilon^2}$, in order to check if our results could be provided by previous analytical results in the literature. For $m=1$ and $a=1$, Hamiltonian (9) is just the truncated Hamiltonian (8) of the CP problem after a normal form expansion or, equivalently, after an averaging process. It should be noted that in the standard application of normal form or averaging, one typically takes $a=0$ because the term $\frac{2a}{3}\varepsilon^2y^3$ is of higher order than the $O(\varepsilon)$ perturbation.
Nevertheless, we found out that the numerically computed values of the splitting depend *essentially* on the parameter a. Particularly the exponent r in formula (7). For the purposes of this paper there are, at least, two different scenarios: the "standard" case $a=0$ and the *new* case $a=1$. Concerning the integrable part of the Hamiltonian (9), for $a=0$ we have a standard pendulum, whereas for $a=1$ we have a new pendulum, that we call *amended pendulum*. See the motivation for including this value of a in Sections 4.2 and 4.3.

6. For $a=0$ there are some theoretical results [28–30] on asymptotics for the splitting of separatrices of general Hamiltonian systems with $1+\frac{1}{2}$ degrees of freedom and fast oscillation in time which are not directly applicable to Hamiltonian (9) which has 2 degrees of freedom. There are no such kind of results available for general Hamiltonians of 2 degrees of freedom with a fast rotor. Nevertheless, in Section 2.5 some general ideas taken from concrete systems [22,23,31,32] are applied to conjecture that the Melnikov prediction with the standard pendulum

$$\Delta p\sim-\varepsilon^m\frac{8\pi}{3}\omega^3\left(1-\frac{2}{\omega^2}\right)\frac{\mathrm{e}^{\pi\omega/2}}{1-\mathrm{e}^{2\pi\omega}} \tag{$*$}$$

(formula (62) in Section 4.1) gives for $m>1$ the correct measure for the splitting for the Toy CP problem (9) with $a=0$. We have numerically confirmed these theoretical results in Section 4.2.
Notice that the exponent of ω in the Melnikov prediction ($*$) for Δp, which is derived (see Section 2.4) for $a=0$, is $r=3$. Therefore ($*$) clearly does not predict the exponent r of ω in (7), as computed numerically in Section 3.3 for the CP problem in resonant coordinates.

7. However, for $a=1$, when we have an *amended pendulum* in Hamiltonian (9), the Melnikov prediction with the amended pendulum coincides with the value (7) of the splitting computed numerically and gives also the right result for $m>1$, both for the exponent r_{CPR} (of ω) and the leading constant A_{CPR}. It is worth noticing that in all formulas the exponential smallness $\mathrm{e}^{\pi\omega/2}$ is the same. This is due to the fact the distance of the closest complex singularity of the separatrices to the real line is the same up to terms of order $\frac{1}{|\omega|}\ln\frac{1}{|\omega|}$, see Appendix C. All these computations are detailed in Section 5 and, in particular, illustrated in Figs. 11 and 12. This is, perhaps, the main novelty of this paper: the normal form or averaging procedure to transform a Hamiltonian system close to a resonance to a nearly integrable Hamiltonian must be carried out at a higher order than initially expected, and choosing uniquely some selected term. In passing, it is worth mentioning that the Melnikov integral is computed numerically, since we do not have an explicit expression for the separatrix of the amended pendulum.

8. From the numerical simulations done, we can conclude that the Toy CP problem with $a=m=1$ is a simplified model that already describes the splitting Δp of the original CP problem in resonant coordinates, as far as asymptotic formulas for Δp, when K tends to zero, are analyzed. See Section 5.3 and, in particular, Fig. 14. Finally, we can also conclude that the fitting asymptotic formula obtained for the Melnikov integral provides the same limit value of the exponent $r_{\text{CPR}}=r_{\text{Mel},1,1}=2.111\ldots=19/9$, where we use $r_{\text{Mel},a,m}$ to denote the exponent of ω in the corresponding Melnikov fitting formula (see (72) in Section 5.1) when Hamiltonian (9) is considered.

9. Along the paper several problems are considered and the associated fitting formulas for the splitting are discussed. In Section 6 we provide two tables (see Tables 3 and 4) with a summary of the results obtained for all the models analyzed.

2. Some analytical computations

2.1. Polar coordinates

The Hamiltonian (1) of the CP problem

$$\mathcal{H}=\frac{1}{2}(p_x^2+p_y^2)-\frac{1}{r}-(xp_y-yp_x)+Kx,\qquad r=\sqrt{x^2+y^2},$$

takes the form in *canonical polar coordinates* (r,θ,p_r,p_θ)

$$H=\frac{1}{2}\left(p_r^2+\frac{p_\theta^2}{r^2}\right)-\frac{1}{r}-p_\theta+Kr\cos\theta:=H_{\text{K}}-p_\theta+Kr\cos\theta.$$

2.2. Delaunay coordinates

We consider the *canonical Delaunay variables* (ℓ, g, L, G), which are the action–angle variables for the Kepler Hamiltonian $H_{\rm K}$ (see [33]). We recall that ℓ is the mean anomaly, g the argument of the pericenter, $a = L^2$ the semimajor axis, $G = p_\theta$ the angular momentum. Other variables are the eccentricity vector $\boldsymbol{e} = (e^{(1)}, e^{(2)}) = (e\cos g, e\sin g)$, the true anomaly $f = \theta - g$ and the eccentric anomaly E. Useful formulas to carry out the change of variables are:

$$\begin{aligned} e &= \sqrt{1-\frac{G^2}{L^2}}, & e^{(2)} &= \left(p_x^2 + p_y^2 - \frac{1}{r}\right) y - (x p_x + y p_y) p_y, \\ \tan\frac{f}{2} &= \sqrt{\frac{1+e}{1-e}} \tan\frac{E}{2}, & \ell &= E - e\sin E, \end{aligned} \tag{10}$$

In the Delaunay variables the Hamiltonian becomes

$$H_D = -\frac{1}{2L^2} - G + K\left(a\cos(\ell+g) - \frac{3}{2}ae\cos g + \frac{ae}{2}\cos(2\ell+g) + O(e^2)\right).$$

2.3. Resonant coordinates

The equilibrium point L_1 satisfies $L = G = 1$ (for $K = 0$). If we introduce the parameter ε as,

$$\varepsilon = \left(\frac{K}{3}\right)^{1/4};$$

then, after changing to resonant variables with a new scaled time $(x, y, \varphi, I; t)$:

$$\ell = x + \pi + \varphi, \qquad g = -\varphi, \qquad L = 1 + \varepsilon^2 y, \qquad G = 1 + \varepsilon^2 y - \varepsilon^2 I; \qquad \tilde{s} = -\frac{t}{3\varepsilon^2}, \tag{11}$$

and averaging (as in [24,25,27,34]), we get the *singular resonant* Hamiltonian

$$H(x, y, \varphi, I; \varepsilon) = \omega I + P_\varepsilon(x, y) + \varepsilon H_1(x, y, \varphi, I; \varepsilon), \tag{12}$$

where

$$\omega = -\frac{1}{3\varepsilon^2},$$

and

$$\begin{aligned} P_\varepsilon(x, y) &= F(y, \varepsilon) + \cos x - 1, \\ H_1(\varphi, x, I, y; \varepsilon) &= \frac{3}{2}\sqrt{2I}\cos\varphi - \frac{1}{2}\sqrt{2I}\cos(2x+\varphi) + O(\varepsilon), \end{aligned}$$

with

$$F(y, \varepsilon) = \frac{y^2}{2} + \frac{f(\varepsilon^2 y)}{3\varepsilon^4} = \frac{y^2}{2} g(\varepsilon^2 y), \tag{13}$$

and

$$\begin{aligned} f(t) &= \frac{1}{2(1+t)^2} - \frac{1}{2} + t - \frac{3}{2}t^2 = -2t^3 + \frac{5}{2}t^4 + \cdots + (-1)^n \frac{n+1}{2} t^n + \cdots = O(t^3), \\ g(t) &= 1 + \frac{2f(t)}{3t^2} = 1 - \frac{4}{3}t + \frac{5}{3}t^2 + \cdots + (-1)^m \frac{m+3}{3} t^m + \cdots. \end{aligned}$$

Taylor expanding in ε we have $F(y, \varepsilon) = F_k(y, \varepsilon) + O\left(\varepsilon^{2k+2} y^{k+3}\right)$, where

$$F_0(y) = \frac{y^2}{2}, \quad F_1(y) = \frac{y^2}{2} - \frac{2}{3}\varepsilon^2 y^3, \quad F_2(y) = \frac{y^2}{2} - \frac{2}{3}\varepsilon^2 y^3 + \frac{5}{6}\varepsilon^4 y^4,$$

and in general

$$F_k(y) = \sum_{n=2}^{k+2} (-1)^n \frac{n+1}{6} \varepsilon^{2n-4} y^n = y^2 \sum_{m=0}^{k} (-1)^m \frac{m+3}{6} \left(\varepsilon^2 y\right)^m, \quad k \geq 0.$$

A remarkable property of this Hamiltonian, for our purposes, is that will allow to distinguish an integrable part with a separatrix plus a perturbation and therefore to apply Melnikov theory. This will be done in the next two subsections.

Further, we introduce new symplectic coordinates (p, q) related with the action I and the angle φ by the change

$$q = \sqrt{2I}\cos\varphi \qquad p = -\sqrt{2I}\sin\varphi \tag{14}$$

so in the coordinates (14), the resonant Hamiltonian (12) casts

$$H_{\text{CPR}}(q, p, x, y; \omega, \varepsilon) = F(y) + V(x) + \omega\frac{q^2+p^2}{2} + \varepsilon H_1(x, y, q, p; \varepsilon), \tag{15}$$

with

$$V(x) = \cos x - 1, \qquad H_1(x, y, q, p; \varepsilon) = \frac{3}{2}q - \frac{q}{2}\cos(2x) - \frac{p}{2}\sin(2x) + O(\varepsilon) \tag{16}$$

(we keep H and H_1 to denote, respectively, the Hamiltonian and perturbation term in these new coordinates, which we also call resonant coordinates).

Remark 1. We notice that the simplest expression — as a perturbation of an integrable Hamiltonian — for the Hamiltonian (15) is

$$H_{\text{CPR}}(q,p,x,y;\omega,\varepsilon)=\frac{y^2}{2}+\cos x-1+\omega\frac{q^2+p^2}{2}+\varepsilon H_1(x,y,q,p;0),$$

2.4. Standard Melnikov prediction for L_1 for ω independent of ε

Now, we consider the Hamiltonian (15) with functions $V(x)$ and $F(y)$ generalized, respectively, to a 2π-periodic potential, $V(x)=V(x+2\pi)$ having a non-degenerate global minimum at $x=0$, so $V(x)=-\lambda^2x^2/2+O(x^3)$, $\lambda>0$, and $F(y)$ to a function having a non-degenerate minimum at $y=0$: $F(0)=F'(0)=0$, $F''(0)=1$. We denote this new (generalized) Hamiltonian by dropping the subindex CPR in (15). Hence,

$$H(x,y,q,p;\omega,\varepsilon)=F(y)+V(x)+\omega\frac{q^2+p^2}{2}+\varepsilon H_1(x,y,q,p;\varepsilon). \tag{17}$$

Furthermore, along this section we are going to assume that ω, $\omega\neq 0$, is independent of ε and we are going to search the so-called "Melnikov prediction" [35,36]. Let us write

$$H_0(x,y,q,p)=F(y)+V(x)+\omega\frac{q^2+p^2}{2}, \tag{18}$$

for the "unperturbed" part of Hamiltonian (17). To distinguish variables it is convenient to introduce

$$u=(x,y),\qquad v=(q,p)$$

to denote the "saddle" coordinates and the "elliptic" or "center" coordinates in (17), respectively. In particular, with this notation the perturbation term can be written as

$$H_1(x,y,q,p;\varepsilon)=H_1(u,v;\varepsilon).$$

We are also going to assume that for the saddle part of Hamiltonian (18)

$$P(x,y)=F(y)+V(x)$$

there exists a *separatrix*

$$u_0(t)=(x_0(t),y_0(t)) \tag{19}$$

contained in $P=0$ satisfying

$$x_0(0)=0,\quad x_0(t)\to 2\pi \text{ for } t\to\infty,\quad x_0(t)\to 0 \text{ for } t\to-\infty,\qquad y_0(t)\to 0 \text{ for } t\to\pm\infty. \tag{20}$$

For instance, the *standard pendulum* has potential energy is $V(x)=\cos x-1$ and kinetic energy $F(y)=\dfrac{y^2}{2}$, which give rise to two *explicit* separatrices

$$x_0(t)=x_0^{\pm}(t)=4\arctan\left(\mathrm{e}^{\pm t}\right),\quad y_0(t)=y_0^{\pm}(t)=\dot{x}_0^{\pm}(t)=\pm\frac{2}{\cosh t}. \tag{21}$$

On the other hand, for the resonant Hamiltonian (15), $V(x)=\cos x-1$ is the potential of a standard pendulum, but the kinetic energy $F(y)$ given in (13) depends essentially on $\varepsilon^2 y$:

$$F(y)=y^2\left(\frac{1}{2}-\frac{2}{3}\varepsilon^2 y+\frac{5}{6}\varepsilon^4y^2+\cdots\right),$$

and we have an *amended pendulum*, which coincides with the standard pendulum only for $\varepsilon=0$, and which has also two separatrices.

For $H_1=0$ the origin $(u,v)=(0,0)$ is a saddle–center equilibrium point with a separatrix (u_0,v_0) satisfying $P(u_0)=0$, $v_0=0$. For $0<|\varepsilon|\ll 1$ there exist stable and unstable invariant manifolds, $W^{\mathrm{s,u}}=\{(u^{\mathrm{s,u}}(t),v^{\mathrm{s,u}}(t))\}$, associated to the new saddle–center $(u^{\mathrm{eq}},v^{\mathrm{eq}})$ which is a critical point of H. Writing

$$\left(u^{\mathrm{eq}},v^{\mathrm{eq}}\right)=\left(\varepsilon u_1^{\mathrm{eq}},\varepsilon v_1^{\mathrm{eq}}\right)+\mathcal{O}\left(\varepsilon^2\right),$$

we get

$$u_1^{\mathrm{eq}}=-\begin{pmatrix}-1/\lambda^2 & 0\\ 0 & 1\end{pmatrix}\nabla_u H_1(0,0;0),\qquad v_1^{\mathrm{eq}}=-\frac{1}{\omega}\nabla_v H_1(0,0;0). \tag{22}$$

To measure the distance between W^{u} and W^{s} we can fix the level of energy of $(u^{\mathrm{eq}},v^{\mathrm{eq}})$ and choose a suitable surface of section just to measure $\Delta v(t):=v^{\mathrm{u}}(t)-v^{\mathrm{s}}(t)$. Notice, on the one hand, that $(u^{\mathrm{s,u}},v^{\mathrm{s,u}})=\left(u_0(t),0\right)$ for $H_1=0$, so we can write $v^{\mathrm{s,u}}(t)=\varepsilon v_1^{\mathrm{s,u}}(t)+\mathcal{O}\left(\varepsilon^2\right)$ and we are going to obtain an explicit formula for $\Delta v_1(t)=v_1^u(t)-v_1^s(t)$. On the other hand, observe that the differential equation satisfied, for example, by $v^{\mathrm{u}}(t)$ is

$$\dot{v}^{\mathrm{u}}=J_2\left(\nabla_v H_0\left(u^{\mathrm{u}},v^{\mathrm{u}}\right)+\varepsilon\nabla_v H_1\left(u^{\mathrm{u}},v^{\mathrm{u}};\varepsilon\right)\right),$$

with $J_2=\begin{pmatrix}0 & 1\\ -1 & 0\end{pmatrix}$. Hence, taking only the first order in ε yields

$$\dot{v}_1^{\mathrm{u}}=J_2\begin{pmatrix}\omega & 0\\ 0 & \omega\end{pmatrix}v_1^{\mathrm{u}}+J_2\nabla_v H_1(u_0(t),0;0)=\omega J_2 v_1^{\mathrm{u}}+J_2\nabla_v H_1(u_0(t),0;0). \tag{23}$$

Besides, we define

$$b(t):=J_2\nabla_v H_1(u_0(t),0;0),$$

notice that then $b(t) \to b_\infty := J_2 \nabla_v H_1(0,0;0)$, when $t \to \pm\infty$. If further, we introduce $\tilde{b}(t) := b(t) - b_\infty$, the system of linear differential equations (23) casts

$$\dot{v}_1^{\mathrm{u}} = \omega J_2 v_1^{\mathrm{u}} + b_\infty + \tilde{b}(t)$$

and clearly we can find the equilibrium point of the autonomous part of this last system by solving $\omega J_2 v_1^u + b_\infty = 0$ to get

$$v_1^{\mathrm{eq}} = -\frac{1}{\omega} \nabla_v H_1(0,0;0)$$

(as in (22)) and introducing $\tilde{v}_1^{\mathrm{u}} = v_1^{\mathrm{u}} - v_1^{\mathrm{eq}}$ we get

$$\dot{\tilde{v}}_1^{\mathrm{u}} = \omega J_2 \tilde{v}_1^{\mathrm{u}} + \tilde{b}(t), \tag{24}$$

with $\tilde{v}_1^{\mathrm{u}}(t) \to 0$ (or $v_1^{\mathrm{u}}(t) \to v_1^{\mathrm{eq}}$) as $t \to -\infty$. Next, solving the linear system of ordinary differential equations (24) by variation of constants one gets

$$\tilde{v}_1^{\mathrm{u}}(t) = \mathrm{e}^{\omega t J_2} \tilde{v}_1^{\mathrm{u}}(0) + \int_0^t \mathrm{e}^{\omega(t-s)J_2} \tilde{b}(s)\, \mathrm{d}s$$

where we stress that $\mathrm{e}^{\omega t J_2} = \begin{pmatrix} \cos\omega t & \sin\omega t \\ -\sin\omega t & \cos\omega t \end{pmatrix} = R(-\omega t)$ is a rotation of angle $-\omega t$. Now, rewriting this solution as

$$R(\omega t)\tilde{v}_1^{\mathrm{u}}(t) = \tilde{v}_1^{\mathrm{u}}(0) + \int_0^t R(\omega s)\, \tilde{b}(s)\, \mathrm{d}s$$

and taking limits $t \to -\infty$ at both sides, the left hand side term clearly goes to zero, so that $\tilde{v}_1^{\mathrm{u}}(0) = \int_{-\infty}^0 R(\omega s)\tilde{b}(s)\, \mathrm{d}s$, and therefore

$$\tilde{v}_1^{\mathrm{u}}(t) = R(-\omega t) \int_{-\infty}^0 R(\omega s)\tilde{b}(s)\, \mathrm{d}s + \int_0^t R\left(\omega(s-t)\right) \tilde{b}(s)\, \mathrm{d}s = \int_{-\infty}^t R\left(\omega(s-t)\right) \tilde{b}(s)\, \mathrm{d}s.$$

Hence $v_1^{\mathrm{u}}(t) = v_1^{\mathrm{eq}} + \int_{-\infty}^t R\left(\omega(s-t)\right) \tilde{b}(s)\, \mathrm{d}s$, or more explicitly,

$$v_1^{\mathrm{u}}(t) = -\frac{1}{\omega} \nabla_v H_1(0,0;0) + \int_{-\infty}^t R\left(\omega(s-t)\right) J_2 \left(\nabla_v H_1(u_0(s),0;0) - \nabla_v H_1(0,0;0) \right) \mathrm{d}s \tag{25}$$

If one should have started from the differential equation satisfied by v^{s}, i.e.,

$$\dot{v}_1^{\mathrm{s}} = J_2 \left(\nabla_v H_0(u^{\mathrm{s}}, v^{\mathrm{s}}) + \varepsilon \nabla_v H_1(u^{\mathrm{s}}, v^{\mathrm{s}}; \varepsilon) \right),$$

having kept, as in (23), only the first order in ε, and proceeded the same way we had done to get (25), one would have arrived to the formula for v_1^{s}, which turns out to be

$$v_1^{\mathrm{s}}(t) = -\frac{1}{\omega} \nabla_v H_1(0,0;0) - \int_t^\infty R\left(\omega(s-t)\right) J_2 \left(\nabla_v H_1(u_0(s),0;0) - \nabla_v H_1(0,0;0) \right) \mathrm{d}s, \tag{26}$$

so that, subtracting (26) to (25), yields

$$\begin{aligned} \Delta v_1(t) &:= v_1^{\mathrm{u}}(t) - v_1^{\mathrm{s}}(t) = \int_{-\infty}^\infty R\left(\omega(s-t)\right) J_2 \left(\nabla_v H_1(u_0(s),0;0) - \nabla_v H_1(0,0;0) \right) \mathrm{d}s \\ &= R(-\omega t)\Delta v_1^0, \end{aligned} \tag{27}$$

where we have introduced

$$\Delta v_1^0 := J_2 \int_{-\infty}^\infty R(\omega s) \left(\nabla_v H_1(u_0(s),0;0) - \nabla_v H_1(0,0;0) \right) \mathrm{d}s.$$

Notice that $\|\Delta v_1(t)\| = \|v_1^{\mathrm{u}}(t) - v_1^{\mathrm{s}}(t)\| = \|v_1^0\|$.

Let us compute this *constant* separation between invariant manifolds for the amended pendulum, that is, for $V(x) = \cos x - 1$, and for a given separatrix $u_0(t) = \left(x_0(t), y_0(t)\right)$ satisfying (20).

Thanks to the even character of the potential $V(x)$, we have the invariance of the amended pendulum under the reversibility $(t,x,y) \mapsto (-t, 2\pi - x, y)$ then, as for small ε the points $\left(\pi, \pm 2 + O\left(\varepsilon^2\right)\right)$ belong to the separatrix, we can take a parameterization of the separatrix (19) such that $\left(x_0^{\pm}(0), y_0^{\pm}(0)\right) = \left(\pi, \pm 2 + O\left(\varepsilon^2\right)\right)$, and hence satisfies

$$\left(x_0(t), y_0(t)\right) = \left(2\pi - x_0(-t), y_0(-t)\right) \tag{28}$$

which, in particular, implies that $\sin\left(x_0(t)\right)$, $\sin\left(2x_0(t)\right)$ are odd in t, and $\cos\left(x_0(t)\right)$, $\cos\left(2x_0(t)\right)$ are even in t. Note that, of course, this is true also for the explicit separatrix of the standard pendulum ($\varepsilon = 0$) given in (21).

In particular, if we consider the perturbation term $H_1(q,p,x,y;\varepsilon)$ given by (16)

$$H_1(x,y,q,p;0) = \frac{3}{2}q - \frac{q}{2}\cos 2x - \frac{p}{2}\sin 2x, \tag{29}$$

one easily gets that

$$R(\omega s) \left(\nabla_v H_1 \left(u_0(s),0;0\right) - \nabla_v H_1\left(0,0;0\right) \right) = \frac{1}{2} \begin{pmatrix} \cos(\omega s) - \cos\left(2x_0(s) + \omega s\right) \\ \sin(\omega s) - \sin\left(2x_0(s) + \omega s\right) \end{pmatrix}.$$

Introducing

$$\mathcal{A}(\omega) := \int_{-\infty}^\infty \mathrm{e}^{\mathrm{i}\omega s} \left(1 - \mathrm{e}^{2\mathrm{i}x_0(s)}\right) \mathrm{d}s, \tag{30}$$

we just get

$$\Delta v_1^0 = \frac{1}{2} J_2 \begin{pmatrix} \mathrm{Re}\mathcal{A}(\omega) \\ \mathrm{Im}\mathcal{A}(\omega) \end{pmatrix} = \frac{1}{2} \begin{pmatrix} \mathrm{Im}\mathcal{A}(\omega) \\ -\mathrm{Re}\mathcal{A}(\omega) \end{pmatrix} = \frac{1}{2} \begin{pmatrix} \displaystyle\int_{-\infty}^{\infty} \left(\sin(\omega s) - \sin\left(2x_0(s) + \omega s\right)\right) \mathrm{d}s \\ \displaystyle -\int_{-\infty}^{\infty} \left(\cos(\omega s) - \cos\left(2x_0(s) + \omega s\right)\right) \mathrm{d}s \end{pmatrix}.$$

and we define $\mathcal{A}^{\pm}(\omega)$ depending on the component $x_0^{\pm}(s)$ of the separatrix chosen.

Taking into account the reversion property (28) of the parameterization we use for the separatrix, it is straightforward to see that $\mathrm{Im}\mathcal{A}(\omega) = 0$, so that $\mathrm{Re}\mathcal{A}(\omega) = \mathcal{A}(\omega)$; that is,

$$\mathcal{A}(\omega) := \int_{-\infty}^{\infty} \left(\cos(\omega s) - \cos\left(2x_0(s) + \omega s\right)\right) \mathrm{d}s, \tag{31}$$

and the difference (27) is just given by

$$\Delta v_1(t) = v_1^{\mathrm{u}}(t) - v_1^{\mathrm{s}}(t) = -\frac{1}{2} R(-\omega t) \begin{pmatrix} 0 \\ \mathcal{A}(\omega) \end{pmatrix}, \tag{32}$$

that is,

$$\Delta q_1(t) := q_1^{\mathrm{u}}(t) - q_1^{\mathrm{s}}(t) = -\frac{1}{2}\mathcal{A}(\omega)\sin\omega t, \qquad \Delta p_1(t) := p_1^{\mathrm{u}}(t) - p_1^{\mathrm{s}}(t) = -\frac{1}{2}\mathcal{A}(\omega)\cos\omega t. \tag{33}$$

Notice that for $t = 0$ the linear approximation of $\Delta p(0)$ is

$$\varepsilon \Delta p_1^{\pm}(0), \qquad \text{with} \qquad \Delta p_1^{\pm}(0) = -\frac{\mathcal{A}^{\pm}(\omega)}{2}. \tag{34}$$

and $\Delta q_1^{\pm}(0) = 0$.

We finish this section to exhibit some explicit computations that can be obtained for the standard pendulum, that is for $F(y) = \frac{y^2}{2}$, where the separatrices have the closed-form expression given in (21), so that $\mathcal{A}^{\pm}(\omega)$ is given by,

$$\begin{aligned} \mathcal{A}^{\pm}(\omega) := \int_{-\infty}^{\infty} \left(\cos(\omega s) - \cos\left(2x_0^{\pm}(s) + \omega s\right)\right) \mathrm{d}s &= \frac{4}{3}\omega^3 \left(1 - \frac{2}{\omega^2}\right) \left[\frac{1}{\cosh\left(\frac{\pi\omega}{2}\right)} \mp \frac{1}{\sinh\left(\frac{\pi\omega}{2}\right)}\right] \\ &= \frac{16\pi}{3}\omega^3 \left(1 - \frac{2}{\omega^2}\right) \frac{\mathrm{e}^{c^{\pm}\pi\omega/2}}{1 - \mathrm{e}^{2\pi\omega}}, \end{aligned} \tag{35}$$

being

$$c^{\pm} = \begin{cases} 1, & \text{for } u^{+}(t), \text{ the external branch } y_0(t) > 0, \\ 3, & \text{for } u^{-}(t), \text{ the internal branch } y_0(t) < 0. \end{cases}$$

See Appendix A for details.

2.5. Averaging and Melnikov method

The main goal of this section is to emphasize the usefulness of the averaging method. In Section 2.3 we have already used it to obtain the resonant Hamiltonian (12), and now we will see how this method allows us to obtain in a direct way the Melnikov integral, which was obtained in Section 2.4 with the help of the variational equations, as well as the error of this averaging approximation. Finally, we will use the averaged equations to study the validity of the Melnikov method for a high frequency ω.

The method developed in the previous section, based on using the variational equations associated with a separatrix to measure the splitting that occurs when a perturbation is added, is commonly known as the *Melnikov method*, or the *Poincaré-Melnikov-Arnold method* in the Hamiltonian case (see [35–37]). In few words, we approximate the system of equations associated to Hamiltonian (17)

$$\begin{aligned} \dot{x} &= F'(y) + \varepsilon \frac{\partial H_1}{\partial y}(x, y, q, p, \varepsilon), \\ \dot{y} &= -V'(x) - \varepsilon \frac{\partial H_1}{\partial x}(x, y, q, p, \varepsilon), \\ \dot{q} &= \omega p + \varepsilon \frac{\partial H_1}{\partial p}(x, y, q, p, \varepsilon), \\ \dot{p} &= -\omega q - \varepsilon \frac{\partial H_1}{\partial q}(x, y, q, p, \varepsilon), \end{aligned} \tag{36}$$

by the simplified system

$$\begin{aligned} \dot{x}_0 &= F'(y_0), \\ \dot{y}_0 &= -V'(x_0), \\ \dot{q}_1 &= \omega p_1 + \varepsilon \frac{\partial H_1}{\partial p}(x_0, y_0, q_1, p_1, 0), \\ \dot{p}_1 &= -\omega q_1 - \varepsilon \frac{\partial H_1}{\partial q}(x_0, y_0, q_1, p_1, 0), \end{aligned} \tag{37}$$

which is just the linear variational equation (23) satisfied by $v_1^{\mathrm{s,u}} = (q_1^{\mathrm{s,u}}, p_1^{\mathrm{s,u}})$ along the separatrix (19). In the previous section we imposed that $v^{\mathrm{s,u}}(t) \to 0$ for $t \to \pm\infty$ and we found formula (27) for the separation $\Delta v_1(t) := v_1^{\mathrm{u}}(t) - v_1^{\mathrm{s}}(t)$ between separatrices. It is worth remarking that the separatrix (19) satisfies the first two equations of system (37), where $F(y)$ may have a whole expansion in the variable ε, as happens in Eq. (13).

To find up to what order in ε we need to expand $F(y)$, it is useful to perform some previous averaging or normalization steps of system (36). Indeed, looking at the particular solutions of system (36) for $\varepsilon = 0$ and $x = y = 0$, which are simply

$$v_0(t) = (q_0(t), p_0(t)) = \left(\sqrt{2I}\cos(\omega t + \varphi), -\sqrt{2I}\sin(\omega t + \varphi)\right),$$

where

$$q_0(0) = \sqrt{2I}\cos\varphi, \qquad p_0(0) = -\sqrt{2I}\sin\varphi, \qquad I = \frac{q_0(t)^2 + p_0(t)^2}{2},$$

we notice that the variables (q_0, p_0) move like an harmonic oscillator, and one can then think about averaging system (36). For instance, for the perturbation H_1 given in Eq. (29), we observe that when we substitute (q, p) by $(q_0(t), p_0(t))$, then $H_1(x, y, q_0(t), p_0(t), 0)$ has zero average with respect to t, and the same happens to its derivatives with respect to x and y. Therefore, averaging system (36) we get system (37).

To find the error of this averaging approximation, we can try to find the change of variables Φ from the Hamiltonian $H = H_0 + \varepsilon H_1$, where $H_0 = \omega I + P$ and $P(x, y) = F(y) + V(x)$, to the averaged Hamiltonian as the 1-time flow of a Hamiltonian εW:

$$\begin{aligned} H\circ\Phi &= H + \{H, \varepsilon W\} + O(\varepsilon^2 W^2) = H_0 + \varepsilon H_1 + \{H_0, \varepsilon W\} + O(\varepsilon^2\ W) \\ &= H_0 + \varepsilon H_1 + \{\omega I, \varepsilon W\} + \{P, \varepsilon W\} + O(\varepsilon^2\ W) = H_0 + \{P, \varepsilon W\} + O(\varepsilon^2\ W), \end{aligned}$$

as long as we solve the so-called *cohomological equation*

$$\{\omega I, W\} + H_1 = 0.$$

For the zero-average perturbation $H_1(x, y, q, p; 0) = \frac{3}{2}q - \frac{q}{2}\cos 2x - \frac{p}{2}\sin 2x$ given in Eq. (29), it is easy to check that

$$W(x, y, q, p) = \left(-\frac{3}{2}p + \frac{p}{2}\cos 2x - \frac{q}{2}\sin 2x\right)\frac{1}{\omega} \tag{38}$$

solves the cohomological equation. Notice that $W = O(1/\omega)$, so that

$$H\circ\Phi = H_0 + \varepsilon\{P, W\} + O(\varepsilon^2/\omega).$$

For $\omega = O(1/\varepsilon^2)$ and $H = H_0 + \varepsilon H_1$, then $W = O(\varepsilon^2)$ and

$$H\circ\Phi = H_0 + \varepsilon\{P, W\} + O(\varepsilon^4) = H_0 + O(\varepsilon^3),$$

so that the approximation

$$F(y) = F_1(y) = \frac{y^2}{2} - \frac{2}{3}\varepsilon^2 y^3,$$

that is, the amended pendulum, is adequate.

As an additional important remark, one can see that the perturbation $\varepsilon\{P, W\}$ can be replaced just by $-\varepsilon H_1$ in the computation of all the Melnikov integrals, as they are evaluated on the separatrix $u_0(t)$.

Indeed, we can write the first-order perturbation H_1 given in (29) and W given in (38) as

$$H_1 = q + \widetilde{H}_1, \qquad W = -\frac{p}{\omega} + \widetilde{W},$$

where $\widetilde{H}_1$ and $\widetilde{W}$ given by

$$\widetilde{H}_1(x, y, q, p; 0) = \frac{q}{2}(1 - \cos 2x) - \frac{p}{2}\sin 2x, \quad \widetilde{W}(x, y, q, p) = \left(-\frac{p}{2}(1 - \cos 2x) - \frac{q}{2}\sin 2x\right)\frac{1}{\omega}$$

satisfy

$$\lim_{t\to\pm\infty}\widetilde{H}_1(x_0(t), y_0(t), q, p; 0) = 0, \qquad \lim_{t\to\pm\infty}\widetilde{W}(x_0(t), y_0(t), q, p) = 0.$$

Denoting by Φ_t^0 the flow of H_0 on the separatrix $\left(x_0(t), y_0(t), q_0(t), p_0(t)\right)$ whereas Φ_t^{00} denotes the flow of H_0 restricted to $x = y = 0$, that is $\left(0, 0, q_0(t), p_0(t)\right)$, from

$$\frac{\mathrm{d}}{\mathrm{d}t}\left(\widetilde{W}\circ\Phi_t^0\right) = \{\widetilde{W}, H_0\}\circ\Phi_t^0$$

one finally gets

$$\int_{-\infty}^{\infty}\{P, W\}\circ\Phi_t^0\,\mathrm{d}t = \int_{-\infty}^{\infty}\{P, \widetilde{W}\}\circ\Phi_t^0\,\mathrm{d}t = \int_{-\infty}^{\infty}H_1\circ\Phi_t^0 - H_1\circ\Phi_t^{00}\,\mathrm{d}t.$$

Similarly one can see that

$$\int_{-\infty}^{\infty}R(\omega t)\,\{P, W\}\circ\Phi_t^0\,\mathrm{d}t = \int_{-\infty}^{\infty}R(\omega t)\left(H_1\circ\Phi_t^0 - H_1\circ\Phi_t^{00}\right)\mathrm{d}t,$$

and an analogous result holds for $\frac{\partial W}{\partial q}$ and $\frac{\partial W}{\partial p}$ instead of W, for instance

$$\int_{-\infty}^{\infty}R(\omega t)\,\nabla_v\{P, W\}\circ\Phi_t^0\,\mathrm{d}t = \int_{-\infty}^{\infty}R(\omega t)\left(\nabla_v H_1\circ\Phi_t^0 - \nabla_v H_1\circ\Phi_t^{00}\right)\mathrm{d}t.$$

We conclude this section by showing how the analysis of the averaged system (37) may be very useful to conjecture the validity of the Melnikov method applied to singular Hamiltonians of the type (12). In fact, we will concentrate on the Toy CP Hamiltonian $H = H_{0,m} = H_0 + \varepsilon^m H_1$ (9) with $a = 0$

$$H_{0,m}(x, y, q, p) = \omega\frac{q^2 + p^2}{2} + \frac{y^2}{2} + \cos x - 1 + \varepsilon^m\left(\frac{3q}{2} - \frac{q}{2}\cos 2x - \frac{p}{2}\sin 2x\right), \ \omega = -\frac{1}{3\varepsilon^2}, \tag{39}$$

to be able to use the well-known singularities of the standard pendulum separatrix.

The averaged system (37) in this case takes the form

$$\begin{aligned} \dot{x}_0 &= y_0,\\ \dot{y}_0 &= \sin x_0,\\ \dot{q} &= \omega p - \frac{\varepsilon^m}{2}\sin 2x_0,\\ \dot{p} &= -\omega q - 3\frac{\varepsilon^m}{2} + \frac{\varepsilon^m}{2}\cos 2x_0, \end{aligned} \tag{40}$$

along the standard pendulum separatrix (21) for $y > 0$

$$x_0(t) = 4\arctan \mathrm{e}^t, \quad y_0(t) = \frac{2}{\cosh t} = x_0'(t) = 2\sin\frac{x_0(t)}{2}.$$

Hamiltonian (39) has a saddle–center behavior at the origin with characteristic exponents ± 1, $\pm \mathrm{i}\omega$ which is weak because the frequency $\omega = -1/3\varepsilon^2$ is fast, and therefore the saddle–center ratio is small: $1/|\omega| = 3\varepsilon^2$. In this kind of analytic systems, the splitting of separatrices is exponentially small, and the standard Poincaré-Melnikov method does not give, *a priori*, the right estimate of its measure, and more refined tools are required, like for instance the study of an associated inner map [30] or a continuous averaging method [38], to study the behavior of the system close to the singularities of the separatrix. Although there are some results about the validation of the Melnikov method for the splitting of separatrices for general Hamiltonians with fast oscillation for $1+1/2$ degrees of freedom [28–30], unfortunately there are no such general results for Hamiltonians with a weak saddle–center with 2-degrees-of-freedom. For concrete cases, in general the Melnikov prediction does not work [22,23], but in some significant concrete problems it gives the right answer [31,32].

In these last cases where the Melnikov prediction provides the right answer, it happens that the behavior of the perturbation close to the singularity of the separatrix is smaller than the behavior of the terms of the unperturbed Hamiltonian close to the separatrix, and this is the criterion that we are going to test.

More precisely, in these singular systems it is crucial to control the values of the terms of the Hamiltonian for times $1/\omega$-close to the singularities of the separatrix. As $\cosh t = \mathrm{i}\sinh(t - \mathrm{i}\pi/2) = \mathrm{i}\sinh\tau$, where $\tau := t - \mathrm{i}\pi/2$, we have that $y_0(t) = -\frac{2\mathrm{i}}{\sinh\tau} \sim -\frac{2\mathrm{i}}{\tau}$ for $\tau \to 0$, as well as a number of asymptotic expressions for $\tau = t - \mathrm{i}\pi/2 \to 0$:

$$\sin x_0(t) = \dot{y}_0(t) \sim \frac{2\mathrm{i}}{\tau^2}, \quad \cos x_0(t) = 1 - \frac{y_0(t)^2}{2} \sim \frac{2}{\tau^2}, \quad \mathrm{e}^{-ix_0(t)} = \cos x_0(t) + \mathrm{i}\sin x_0(t) \sim \frac{4}{\tau^2},$$

$$\mathrm{e}^{ix_0(t)} = \frac{1}{\mathrm{e}^{-ix_0(t)}} \sim \frac{\tau^2}{4}, \quad \mathrm{e}^{2ix_0(t)} \sim \frac{\tau^4}{16}, \quad \mathrm{e}^{-2ix_0(t)} \sim \frac{16}{\tau^4}, \quad \sin 2x_0(t) = 2\sin x_0(t)\cos x_0(t) \sim \frac{8\mathrm{i}}{\tau^4}.$$

On the one hand, along the separatrix, H_0 contains the terms $\frac{y_0^2(t)}{2} \sim \frac{-2}{\tau^2}$ and $\cos x_0(t) = 1 - \frac{y_0^2(t)}{2} \sim \frac{2}{\tau^2}$ so that, for $\tau \sim \varepsilon^2$, we have that

$$H_0 \sim \varepsilon^{-4}. \tag{41}$$

On the other hand, H_1 can be written as

$$H_1 = \frac{3q}{2} - \frac{1}{4}(q - \mathrm{i}p)\,\mathrm{e}^{2\mathrm{i}x} - \frac{1}{4}(q + \mathrm{i}p)\,\mathrm{e}^{-2\mathrm{i}x}.$$

From (40) we have that

$$(q - \mathrm{i}p)^{\cdot} = i\omega(q - \mathrm{i}p) + \mathrm{i}\frac{3}{2}\varepsilon^m - \mathrm{i}\frac{\varepsilon^m}{2}\,\mathrm{e}^{-2\mathrm{i}x_0} \sim -\frac{8i\varepsilon^m}{\tau^4},$$

from which $q - \mathrm{i}p \sim \frac{8i\varepsilon^m}{3\tau^3}$. Analogously, from

$$(q + \mathrm{i}p)^{\cdot} = -i\omega(q + \mathrm{i}p) - \mathrm{i}\frac{3}{2}\varepsilon^m + \mathrm{i}\frac{\varepsilon^m}{2}\,\mathrm{e}^{2\mathrm{i}x_0} \sim -i\omega(q + \mathrm{i}p) - \mathrm{i}\frac{3}{2}\varepsilon^m,$$

we get $q + \mathrm{i}p \sim -\frac{3\varepsilon^m}{2\omega} = \varepsilon^{m+2}$. In a similar way $\dot{q} \sim -\frac{4\mathrm{i}\varepsilon^m}{\tau^4}$ implies $q \sim +\frac{4\mathrm{i}\varepsilon^m}{3\tau^3}$.

If we plug these three asymptotic expressions into the expression of H_1 for $\tau \sim \varepsilon^2$, we get

$$\varepsilon^m H_1 \sim \varepsilon^{2m-6}. \tag{42}$$

Comparing with the estimate of the unperturbed Hamiltonian H_0 of (41), the size of the perturbation $\varepsilon^m H_1$ of (42) will be smaller when $\varepsilon^{2m-6} \ll \varepsilon^{-4}$, that is, for $m > 1$, which is the exponent for which we can expect that the Melnikov method will give the right answer.

The case $m = 1$ is the so-called limit o singular case [30], where the constant A may require the use of the inner equation as in [22,23,29,30] to provide the right answer.

3. Numerical results. Splitting of the invariant manifolds of L_1, $W^{u,s}(L_1)$

In this part of the paper we discuss the methodology used and the results obtained from numerical computations.

3.1. Numerical computation of the manifolds $W^{u,s}(L_1)$ of the equilibrium point L_1

Our first goal is to compute $W^{u,s}(L_1)$ numerically. An effective way to so is applying the parameterization method (shortly reminded in Appendix B) in order to obtain high order expansions of $W^{u,s}(L_1)$. Moreover, since we will need to deal with very small values of K to check exponentially small estimates for the splitting between $W^u(L_1)$ and $W^s(L_1)$, a multiple precision arithmetic will be required. Also regarding the numerical

computations, we observe that using the Hamiltonian for the CP problem in synodical coordinates $(x, y, \dot{x}, \dot{y})$ implies a term $1/r^3$ in the ODE. To make the computations more efficient, we will change to Levi-Civita coordinates (u, v, u', v') and a new time τ (with $' = \mathrm{d}/\mathrm{d}\tau$) defined by

$$x = u^2 - v^2, \qquad y = 2uv, \qquad \frac{\mathrm{d}t}{\mathrm{d}\tau} = 4(u^2 + v^2) \tag{43}$$

so the system of ODE now becomes

$$\begin{cases} u'' - 8(u^2 + v^2)v' = -4Cu - 16Ku^3 + 12(u^2 + v^2)^2 u, \\ v'' + 8(u^2 + v^2)u' = -4Cv + 16Kv^3 + 12(u^2 + v^2)^2 v, \end{cases}$$

where C is given by (5) and $' = \mathrm{d}/\mathrm{d}\tau$, which is simply polynomial, and the implementation of the parameterization method becomes simpler and more efficient.
We recall that:

1. The Levi-Civita transformation (43) duplicates the configuration plane.

2. There exists a first integral expressed by

$$u'^2 + v'^2 = 8(u^2 + v^2)\left(\frac{1}{2}(u^2 + v^2)^2 + \frac{1}{u^2 + v^2} - K(u^2 - v^2) - \frac{C}{2}\right)$$

which is regular everywhere (including the collision $u = v = 0$).

3.2. Splitting in synodic coordinates

The next step consists of computing the distance between the unstable and stable invariant manifolds associated with L_1 at some Poincaré section Σ, which is taken as $y = 0$, $x > 0$ (or correspondingly to $v = 0$, $u > 0$ in Levi-Civita coordinates). We will focus on the external manifolds $W^{\mathrm{u,e}}$ and $W^{\mathrm{s,e}}$ (see Fig. 2), and from now on we simply denote them by W^{u} and W^{s}. Fixed a value of $K > 0$, we want to compute the distance — also called the splitting — between W^u and W^s at the first crossing with Σ, that is the distance between the two points $P^u = (x^u, y^u, p_x^u, p_y^u)$ and $P^s = (x^s, y^s, p_x^s, p_y^s)$, with $y^u = y^s = 0$ (we will provide the splitting for the variables (x, y, p_x, p_y) although the numerical simulations will be done using Levi-Civita coordinates). However notice that due to the symmetry (3), $x^u = x^s$, $p_y^u = p_y^s$ and $p_x^s = -p_x^u$, the stable manifold W^{s} does not need to be computed and the distance between P^u and P^s is simply $2p_x^u = 2\dot{x}^u := \Delta\dot{x}$, since $p_x = \dot{x} - y = \dot{x}$ at Σ (of course the corresponding reversibility applies in Levi-Civita coordinates).

Next, for different values of K we compute the corresponding value $\Delta\dot{x}$. We have taken a range of values of K decreasing from 0.001 to 10^{-8}.

Our next purpose is to fit the resulting data by an asymptotic formula. To do so, we start with a *naive* fit, that is a formula $\Delta\dot{x} \sim c \cdot \exp(\omega d)$, or equivalently $\ln \Delta\dot{x} \sim \ln c + d \ln|\omega|$, where $\omega = -\dfrac{1}{3\varepsilon^2}$ and we look for the constant d. Using divided differences we obtain that $d = \pi/2$. The next fit asymptotic formula (inspired in formulas (34) and (35)) is

$$\Delta\dot{x} \sim \varepsilon A|\omega|^r \exp\left(\frac{\omega\pi}{2}\right) \tag{44}$$

or equivalently

$$\ln|\Delta\dot{x}| - \ln\varepsilon - \frac{\omega\pi}{2} \sim \ln A + r\ln|\omega|. \tag{45}$$

The crucial point is to determine the values of $\ln A$ and r. To do so, we have proceeded following three strategies:

(i) from the output data $(K, \Delta\dot{x})$, we plot the points $(\ln|w|, Y_{\Delta\dot{x}})$ where $Y_{\Delta\dot{x}} = \ln|\Delta\dot{x}| - \ln\varepsilon - \dfrac{\omega\pi}{2}$ –see Fig. 3–. We clearly see that the points lie on a line. Actually, a linear regression approximation using formula (45) provides

$$r = r_{\mathrm{CP}} = 1.6115, \qquad \ln A = \ln A_{\mathrm{CP}} = 2.772, \qquad A = A_{\mathrm{CP}} = 15.99058.$$

(ii) Since formulas (44) or (45) are asymptotic formulas, it seems quite reasonable to take for each pair of points $(K_i, \Delta\dot{x}_i)$ and $(K_{i+1}, \Delta\dot{x}_{i+1})$, the segment passing through the points $(\ln|\omega_i|, Y_{\Delta\dot{x}_i})$ and $(\ln|\omega_{i+1}|, Y_{\Delta\dot{x}_{i+1}})$ and look at the tendency of the slope of such segments when K decreases. We associate to this segment the expression $r\ln|\omega| + \ln A$ and we plot the obtained values of r in Fig. 4 left and the obtained values of $\ln A$ in the right figure. For the last pair of points we obtain

$$r = r_{\mathrm{CP}} = 1.6114670\ldots, \qquad \ln A = \ln A_{\mathrm{CP}} = 2.7726505\ldots, \qquad A = A_{\mathrm{CP}} = 16.000988\ldots, \tag{46}$$

which are very similar values to those obtained in strategy *(i)*.

A remark must be done at this point: notice that the decreasing values of K considered range from 0.001 to 10^{-8}, or correspondingly the range of increasing values in $\ln|w|$ is from 2.8 to 8.6. However the range of values in ε is from 0.14 to 0.0076, which turns out to be poor. Nevertheless, we emphasize that the numerical computations have been done using multiple precision arithmetics dealing with up to five thousand digits and a high order for the parameterization. So we reach a limit computing capacity for taking smaller values of K, and therefore smaller values of ε.

(iii) Actually, using an extrapolation approach, formula (44) can be written as

$$\Delta\dot{x} \sim \varepsilon|\omega|^r \exp\left(\frac{\omega\pi}{2}\right)\left(A + A_1\varepsilon^{j_1} + A_2\varepsilon^{j_2} + \cdots\right)$$

or equivalently as

$$Z_{\Delta\dot{x}} := \frac{1}{\varepsilon}|\omega|^{-r}\Delta\dot{x}\exp\left(-\frac{\omega\pi}{2}\right) \sim A + A_1\varepsilon^{j_1} + A_2\varepsilon^{j_2} + A_3\varepsilon^{j_3} + \cdots \tag{47}$$

and our goal is to obtain an (as much precise as possible) value of A, once r is given. Although we do not know the exact value of r, from the numerical computations done in next Sections for the perturbed pendulum and for the perturbed amended pendulum, we will show (later on) that the *guess* value for $r = r_{\mathrm{CP}}$ is $r_{\mathrm{CP}} = 1.611111\ldots = 29/18$.

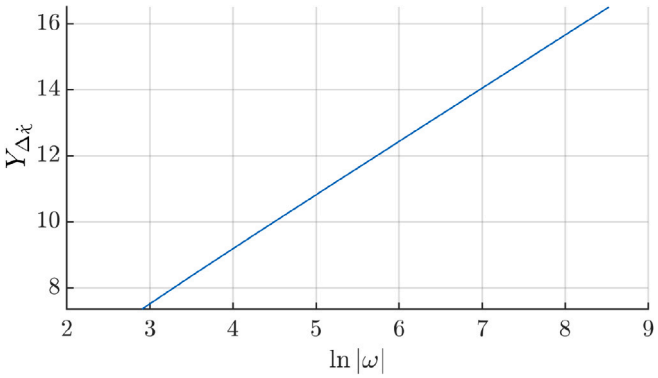

Fig. 3. Points $(\ln|\omega|, Y_{\Delta\dot{\chi}})$ varying (decreasing to zero) K (or equivalently increasing $\ln|\omega|$). Notice the points *lying* on the line $Y = 2.772 + 1.6115\ln|\omega|$.

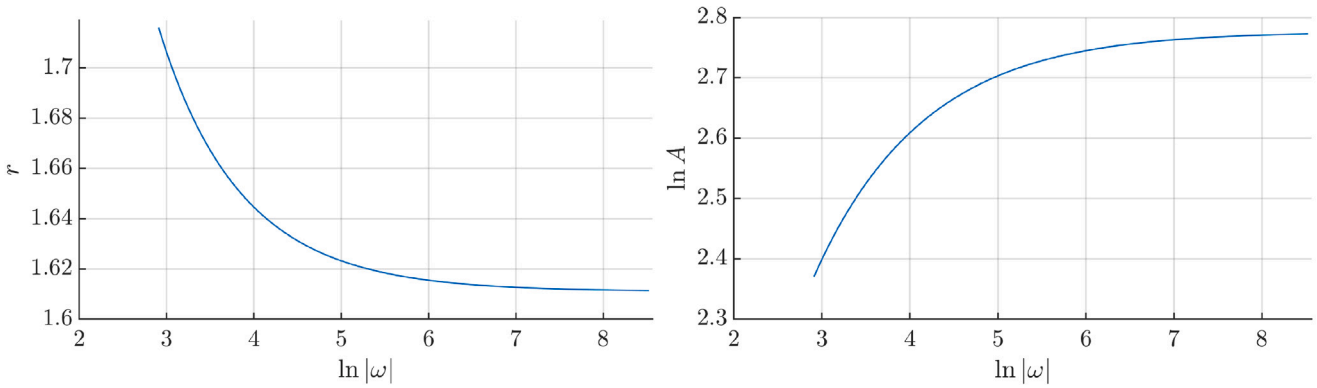

Fig. 4. Values of r (left) and $\ln A$ (right) obtained when taking pairs of points $(K_i, \Delta\dot{\chi}_i)$ and $(K_{i+1}, \Delta\dot{\chi}_{i+1})$ varying (decreasing to zero) K (or equivalently increasing $\ln|\omega|$). See the text for details.

Table 1
Approximate values of $A = A_{\text{CP}}$ in formula (47) obtained by extrapolation.

K	ε	$Z_{\Delta\dot{\chi}}$	1st extrapolation	2nd extrapolation
1.432E−8	8.312E−3	**16.0493**664120828	**16.055307**49436553	**16.0553078439**006
1.419E−8	8.293E−3	**16.0493**937101860	**16.055307**49756964	**16.0553078438**344
1.406E−8	8.274E−3	**16.0494**208816007	**16.055307**50074373	**16.0553078437**819
1.393E−8	8.255E−3	**16.0494**479266667	**16.055307**50388795	**16.0553078437**170
1.380E−8	8.236E−3	**16.0494**748478517	**16.055307**50700268	**16.0553078436**392
1.367E−8	8.217E−3	**16.0495**016497992	**16.055307**51008853	**16.0553078435**483
1.355E−8	8.198E−3	**16.0495**283244532	**16.055307**51314551	**16.0553078433**730
1.342E−8	8.179E−3	**16.0495**548764688	**16.055307**51617363	**16.0553078434**478
1.330E−8	8.160E−3	**16.0495**813084435	**16.055307**51917351	**16.0553078433**717
1.318E−8	8.141E−3	**16.0496**076165450	**16.055307**52214528	**16.0553078433**357

Using formula (47) we have done several steps of extrapolation to obtain a robust value of $A = A_{\text{CP}}$ (using the last 50 values of K close to 10^{-8}) (see values of (K, ε) in Table 1, where only the smallest 10 values of K are shown). That is, we have taken values of $(\varepsilon, Z_{\Delta\dot{\chi}})$ (see column 2 and 3 in the table) and after some attempts, varying the values of j_i, we conclude that we get the best fit of A_{CP} with $j_i = 2 \cdot i$ and the value of A_{CP} is $A_{\text{CP}} = 16.055307843$ (or $\ln A_{\text{CP}} = 2.776039450$). See columns 3, 4, 5 in the table. Columns 4 and 5 have been obtained taking the first two extrapolation steps.

In summary, with the data at hand the specific values of A and r turn out to be

$$A = A_{\text{CP}} = 16.055307843\ldots \ (\ln A = \ln A_{\text{CP}} = 2.77603950\ldots), \ r = r_{\text{CP}} = 1.6111111\ldots = 29/18. \tag{48}$$

3.3. Splitting in resonant coordinates

Motivated, on one hand, by formulas (35) and (34) at $t = 0$ which provide explicit expressions of the splitting for the standard perturbed pendulum, and on the other hand, by the numerical simulations done in the previous subsection, we want to analyze the splitting (distance between the external manifolds $W^{u,e}$ and $W^{s,e}$ at the Poincaré section Σ) when taking into account, not the original variables (χ, y, p_χ, p_y) but the resonant ones (x, y, p, q). So, for each value of K, once we obtain the point P^u from the computations described in the previous subsection for the CP problem, we apply the change of coordinates from Levi-Civita (u, v, u', v') to synodical ones (χ, y, p_χ, p_y) and to resonant coordinates (x, y, p, q), so now P^u becomes (x^u, y^u, q^u, p^u), with $x^u \approx \pi$. Taking the same range of values of K tending to zero, more precisely a set of values K_i, $i = 1, \ldots, N$

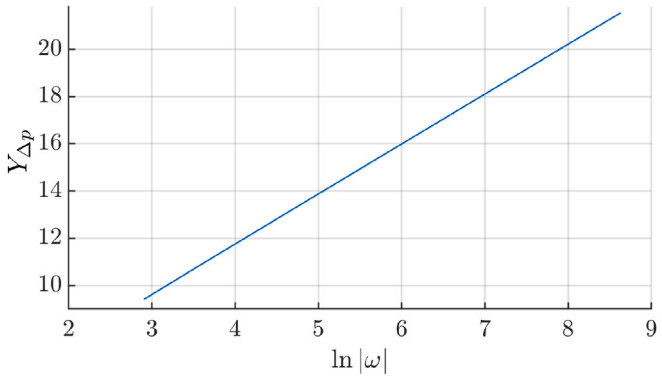

Fig. 5. Points $(\ln|\omega|, Y_{\Delta p})$ varying (decreasing to zero) K (or equivalently increasing $\ln|\omega|$). Notice the points *lying* on the line $Y = 3.325 + 2.111\ln|\omega|$.

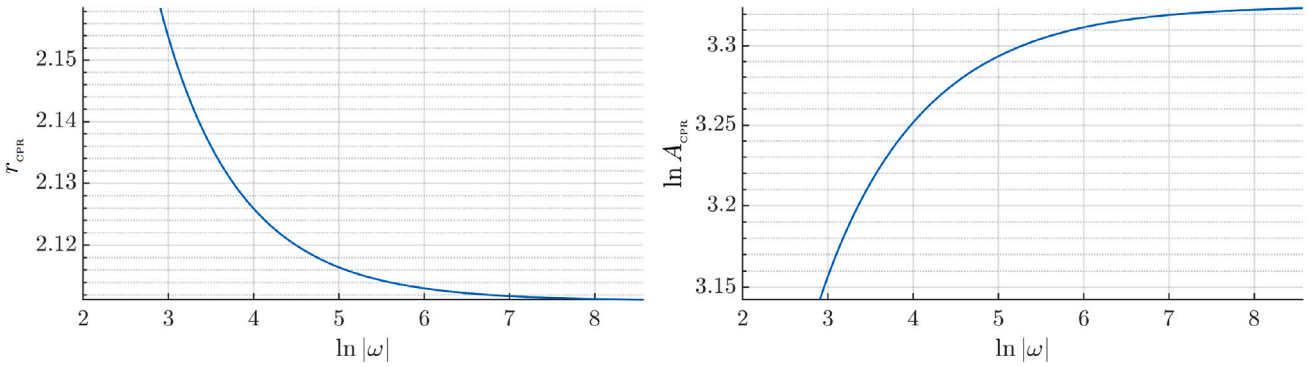

Fig. 6. Values of r_{CPR} (left) and $\ln A_{\text{CPR}}$ (right) obtained when taking pairs of points $(K_i, \Delta p_i)$ and $(K_{i+1}, \Delta p_{i+1})$, in resonant coordinates, varying (decreasing to zero) K (or equivalently increasing $\ln|\omega|$). See the text for details.

with $K \in [10^{-8}, 10^{-3}]$ and using multiple precision computations, we compute the splitting which now we define as $\Delta p = 2p^u.$ to π). Taking into account formulas (34) and (35), where we skip the + notation since we only consider the external manifolds, we fit the splitting by the asymptotic formula

$$|\Delta p| \sim \varepsilon A|\omega|^r \exp\left(\frac{\omega\pi}{2}\right) \tag{49}$$

or equivalently

$$\ln|\Delta p| - \ln\varepsilon - \frac{\omega\pi}{2} \sim \ln A + r\ln|\omega|. \tag{50}$$

Our next goal is to determine $A = A_{\text{CPR}}$ and $r = r_{\text{CPR}}$. We proceed applying the three strategies mentioned above.

(i) We plot the points $(\ln|\omega|, Y_{\Delta p})$, with $Y_{\Delta p} := \ln|\Delta p| - \ln\varepsilon - \frac{\omega\pi}{2}$, see Fig. 5. Again we observe the good fit of points $(\ln|\omega|, Y_{\Delta p})$ by a line. A linear regression approximation using formula (50) provides $\ln A_{\text{CPR}} = 3.325$ and $r_{\text{CPR}} = 2.111$.

(ii) Taking each successive pair of points $(K_i, \Delta p_i)$ and $(K_{i+1}, \Delta p_{i+1})$ and the segment passing through the points $(\ln|\omega_i|, Y_{\Delta p_i})$ and $\left(\ln|\omega_{i+1}|, Y_{\Delta p_{i+1}}\right)$. We associate to this segment the expression $r\ln|\omega| + \ln A$ and we plot the obtained values of $r = r_{\text{CPR}}$ in Fig. 6 left, and the obtained values of $\ln A = \ln A_{\text{CPR}}$ in the right figure. With the data at hand, the last values obtained for $\ln A_{\text{CPR}}$ and r_{CPR} are $\ln A_{\text{CPR}} = 3.323854\ldots$, $r_{\text{CPR}} = 2.111267\ldots$, which are very similar to those values in strategy *(i)*.

(iii) We now make use of the fit formula

$$|\Delta p| \sim \varepsilon|\omega|^r \exp\left(\frac{\omega\pi}{2}\right)\left(A + A_1\varepsilon^{j_1} + A_2\varepsilon^{j_2} + \ldots\right),$$

or equivalently as

$$Z_{\Delta p} := \frac{1}{\varepsilon}|\omega|^{-r}|\Delta p|\exp\left(-\frac{\omega\pi}{2}\right) \sim A + A_1\varepsilon^{j_1} + A_2\varepsilon^{j_2} + A_3\varepsilon^{j_3} + \ldots \tag{51}$$

and as we have done previously with $\Delta\dot{x}$, we want to apply extrapolation to obtain an (as much precise as possible) value of $A = A_{\text{CPR}}$, once $r = r_{\text{CPR}}$ is given. Again, we need a guess value which turns out to be $r_{\text{CPR}} = 2.11111\ldots = 19/9$. This value will be justified in Section 5.

Using formula (51) we have done two steps of extrapolation to obtain a robust value of A_{CPR} (again using the same last 50 values of K close to 10^{-8}, see Table 2) where we have taken $j_i = 2\cdot i$ (which provides the best fit). We list the values of A_{CPR} obtained through the successive extrapolation steps (we only provide the last 10 values but we have used 50):

In summary, with the data at hand, the values of A_{CPR} and r_{CPR} turn out to be

$$A_{\text{CPR}} = 27.80860891\ldots \quad (\ln A_{\text{CPR}} = 3.325345645\ldots), \qquad r_{\text{CPR}} = 2.11111\ldots = 19/9, \tag{52}$$

Table 2
Approximate values of $A = A_{\text{CPR}}$ in formula (51) obtained by extrapolation.

$Z_{\Delta p}$	1st extrapolation	2nd extrapolation
27.8040812616518	**27.80860932094579**	**27.8086089**167525
27.8041020671644	**27.80860931723887**	**27.8086089**166344
27.8041227760921	**27.80860931356489**	**27.8086089**165020
27.8041433886943	**27.80860930992373**	**27.8086089**163859
27.8041639068522	**27.80860930631499**	**27.8086089**162863
27.8041843341052	**27.80860930273799**	**27.8086089**162036
27.8042046643138	**27.80860929919275**	**27.8086089**160301
27.8042249010261	**27.80860929567928**	**27.8086089**159491
27.8042450462224	**27.80860929219689**	**27.8086089**158544
27.8042650969822	**27.80860928874547**	**27.8086089**157148

Remark. We notice that the Poincaré section $y = 0$ does not correspond to $x = \pi$ but $x = \pi + \delta$. However, numerical computations reveal that

$$\delta = C\varepsilon^2 |\omega|^{r_{\text{CPR}}} \exp\left(\frac{\omega\pi}{2}\right)$$

so in terms of comparison of the fit formulas for the splitting, we can deal with the Poincaré section $x = \pi$ or $x = \pi + \delta$, indistinctly (since the contribution of δ is of order ε^2, apart from the exponentially small term).

At this point, two natural questions arise: *(i)* Can we explain the difference between $r_{\text{CP}} = 1.611\ldots$ and $r_{\text{CPR}} = 2.111\ldots$ and the difference between A_{CP} and A_{CPR}? *(ii)* Does the Melnikov theory predict the asymptotic formula (49) or (50) with these values of r_{CPR} and $\ln A_{\text{CPR}}$? Next section is devoted, in particular, to answer the second question. Concerning the first question, let us prove the following result:

At the Poincaré section $\Sigma : y = 0$, we have

$$\dot{x} \approx -\varepsilon p$$

or equivalently,

$$\Delta\dot{x} \approx -\varepsilon \Delta p.$$

To prove this assertion, let us assume that $x = 1 + O(\delta)$, $y = O(\delta)$, and $\dot{x} > 0$ being δ a small quantity. Then using formulas (10)

$$\begin{aligned} a &= \frac{x}{2 - x(\dot{x}^2 + y^2) - 2y x^2 - x^3} = \frac{1 + O(\delta)}{2 - (1 + O(\delta))(\dot{x}^2 + O(\delta^2)) - 2O(\delta^2) - 1 + O(\delta)} \\ &= \frac{1 + O(\delta)}{1 - \dot{x}^2(1 + O(\delta)) + O(\delta)} = \frac{1 + O(\delta)}{1 - \dot{x}^2 + O(\delta)} \\ &= \frac{1}{1 - \dot{x}^2} + O(\delta), \\ L &= \frac{1}{\sqrt{1 - \dot{x}^2}} + O(\delta) \\ G &= x(y + x) = 1 + O(\delta) \end{aligned}$$

so

$$L - G = \frac{\dot{x}^2}{\sqrt{1 - \dot{x}^2} + 1 - \dot{x}^2} + O(\delta)$$

and

$$\begin{aligned} \sqrt{2(L - G)} &= \frac{\sqrt{2}\dot{x}}{\sqrt{\sqrt{1 - \dot{x}^2} + 1 - \dot{x}^2}} + O(\delta) \\ e &= \sqrt{1 - \frac{G^2}{a}} = \dot{x} + O(\delta). \end{aligned}$$

Moreover recall from the eccentricity vector $\mathbf{e} = (e^{(1)}, e^{(2)})$ that $e^{(2)} = -x\dot{x}(y + x) = -\dot{x} + O(\delta)$. So finally

$$p = \frac{\sqrt{2(L - G)}}{\varepsilon} \sin g = \frac{\sqrt{2(L - G)}}{\varepsilon} \frac{e^{(2)}}{e} \approx \frac{1}{\varepsilon}\dot{x},$$

that is

$$\dot{x} \approx -\varepsilon p. \tag{53}$$

Expression (53) allows us to relate the exponent r_{CP} and r_{CPR} and the constants A_{CP} and A_{CPR} in the two fit formulas:

$$\Delta\dot{x} = 2\dot{x} \sim A\varepsilon|\omega|^r \exp\left(\frac{\omega\pi}{2}\right), \quad \text{with} \quad r = r_{\text{CP}} = 1.61111\ldots = \frac{28}{19}, \ A = A_{\text{CP}} = 16.0553078\ldots \tag{54}$$

$$\Delta p = 2|p| \sim A\varepsilon|\omega|^r \exp\left(\frac{\omega\pi}{2}\right), \quad \text{with} \quad r = r_{\text{CPR}} = 2.1111\ldots = \frac{19}{9}, \ A = A_{\text{CPR}} = 27.8086089\ldots. \tag{55}$$

Indeed, using $|\dot{\chi}| = \varepsilon|p|$, we obtain

$$r_{\text{CPR}} = r_{\text{CP}} + \frac{1}{2}, \qquad A_{\text{CP}} \approx \frac{A_{\text{CPR}}}{\sqrt{3}}, \tag{56}$$

which agrees with the relation $r_{\text{CPR}} = 2.11111\ldots = 1.611111 + 0.5 = r_{\text{CP}} + 0.5$ and the numerical values of A_{CP} and A_{CPR} obtained in (54) and (55) (we precisely get $\frac{A_{\text{CPR}}}{\sqrt{3}} = 16.0553078\ldots$ which coincides with the value of A_{CP} up to the first 9 digits).

4. The perturbed standard pendulum. Other possible models

This Section is devoted to answer the following question: does the Melnikov theory predict the asymptotic formula (49) with these values of r_{CPR} and $\ln A_{\text{CPR}}$?

To answer this question we take, as the most natural model, the first order in ε Hamiltonian. More precisely, in Section 2.3 we have written the Hamiltonian of the CP problem in resonant coordinates (x, y, q, p) (see (17)). We now consider the Hamiltonian as an expansion in powers of $\varepsilon = (K/3)^{1/4}$:

$$\begin{aligned} H &= \omega\frac{q^2+p^2}{2} + \frac{y^2}{2} + \cos x - 1 + \varepsilon\left[\frac{3}{2}q - \frac{q}{2}\cos 2x - \frac{p}{2}\sin 2x\right] \\ &\quad + \varepsilon^2\left[\left(-\frac{3}{8}q^2 - \frac{5}{8}p^2\right)\cos x + 2y\cos x + \frac{1}{4}qp\sin x + \frac{3}{8}\left(q^2-p^2\right)\cos 3x + \frac{3}{4}qp\sin 3x - \frac{2}{3}y^3\right] + \cdots \\ &:= H_0 + \varepsilon H_1 + \varepsilon^2 H_2 + \cdots \end{aligned} \tag{57}$$

and we take as the simplest model the first order expansion,

$$H_{0,1}(x, y, q, p) = H_0(x, y, q, p) + \varepsilon H_1(x, y, q, p) \tag{58}$$

with

$$H_0(x, y, q, p) = \omega\frac{q^2+p^2}{2} + \frac{y^2}{2} + \cos x - 1 \tag{59}$$

and

$$H_1(x, y, q, p) = \frac{3}{2}q - \frac{q}{2}\cos 2x - \frac{p}{2}\sin 2x, \tag{60}$$

and we call (58) the perturbed standard pendulum (although H_0 is a rotor times a standard pendulum).

At this point we remark that Hamiltonian (58) can be regarded as a particular case of the more general Hamiltonian

$$H_{0,m}(x, y, q, p) = H_0(x, y, q, p) + \varepsilon^m H_1(x, y, q, p) \tag{61}$$

with H_0 and H_1 given by (59) and (60) respectively.

Actually in this Section we want to test the Melnikov theory for the more general Hamiltonian (61), $m \geq 1$, from which $m = 1$ — that is Hamiltonian (58) corresponding to a natural approximation of the CP problem — is a particular case.

So, we consider the general Hamiltonian (61) and we proceed as follows: (i) we compute the Melnikov integral for the separatrix. Notice that a clear advantage of this Hamiltonian is that we know the explicit expression of the separatrices (given by (21)) in $(q, p) = (0, 0)$ of the integrable Hamiltonian $H_0(x, y, q, p)$, which is a rotor times a pendulum. An immediate consequence of this Melnikov integral computation will provide the answer to our initial question in this Section: the theoretical Melnikov prediction does not provide the expected values r_{CPR} and A_{CPR}. (ii) Going on with the general Hamiltonian $H_{0,m}$, we observe that the associated system of ODE has two equilibrium points: $L_- = (0, 0, 3\varepsilon^{2+m}, 0)$ and $L_+ = (2\pi, 0, 3\varepsilon^{2+m}, 0)$. We will focus our attention on the external unstable manifold of L_- (that will start describing a curve in the (x, y) projection with $y > 0$, $x > 0$), and the external stable manifold of L_+ (that will start describing a curve in the (x, y) projection with $y > 0$, $x < 2\pi$). We want to measure the distance between them (the splitting) at a given Poincaré section. Due to the symmetry $(x, y, q, p, t) \to (2\pi - x, y, q, -p, -t)$ satisfied by the associated system of ODE, a Poincaré section that turns out to be convenient is $\widetilde{\Sigma} : x = \pi, y > 0$. From now on we will omit the *external* mention when discussing the manifolds and we will simply refer to them as the manifolds. (iii) We will compute the splitting between $W^u(L_-)$ and $W^s(L_+)$ at $\widetilde{\Sigma}$, which will be denoted by Δp (see details on the notation below). (iv) We will fit Δp by some suitable asymptotic formula. (v) We will check if for any value of $m \geq 1$, the Melnikov integral formula predicts the asymptotic behavior provided by the previous fitting formula. In the sequel we detail the computations.

4.1. Melnikov integral for the perturbed standard pendulum

Formula (35) provides the Melnikov integral for the separatrix of the standard pendulum and Formula (33) provides (the linear approximation of) the splitting. In particular at $t = 0$ we have

$$\Delta p \sim -\varepsilon^m \frac{8\pi}{3}\omega^3\left(1 - \frac{2}{\omega^2}\right)\frac{e^{\pi\omega/2}}{1 - e^{2\pi\omega}}, \tag{62}$$

with $m = 1$ (obviously the same formula is obtained for a Hamiltonian $H_0(x, y, q, p) + \varepsilon^m H_1(x, y, q, p)$). So, comparing the splitting fit formulas (49) and (62) we obtain $r = 3$ from Melnikov formulation, instead of the expected value $r_{\text{CPR}} = 2.111\ldots$ and $A = \frac{8\pi}{3} = 8.377\ldots$ instead of $A_{\text{CPR}} = 27.808\ldots$ (see (52)). We can conclude that the numerical results for Δp do not coincide with the theoretical prediction given by the Melnikov formula.

4.2. Analysis of the toy CP problem with $a = 0$

Although the Hamiltonian $H_{0,1}$ in (58) turns out not to be a good approximation to get the asymptotic fit for Δp for the CP problem, it is interesting to analyze the following Hamiltonian — per se and to compare our results with previous ones in the literature —, taking the same integrable part plus a more general perturbation, that is the Toy CP problem with $a = 0$,

$$H_{0,m}(x, y, q, p) = H_0(x, y, q, p) + \varepsilon^m H_1(x, y, q, p) \tag{63}$$

where $m \geq 1$, H_0 and H_1 are given by (59) and (60). Let us recall that from the analysis performed in the previous Section 2.5, for $m > 1$ one expects that Melnikov prediction with the standard pendulum would provide the correct measure (62) for the splitting.

Let us consider the equilibrium points of $H_{0,m}$. As mentioned above, they are $L_- = (0, 0, 3\varepsilon^{2+m}, 0)$ and $L_+ = (2\pi, 0, 3\varepsilon^{2+m}, 0)$. Our goal, in this subsection, is to check if the splitting between the unstable manifold of L_- (in $y \geq 0$) and the stable manifold of L_+ (in $y \geq 0$) measured at the Poincaré section $\widetilde{\Sigma}$ defined by $x = \pi$, $y > 0$, can be predicted by the Melnikov formula (32) obtained analytically regardless the value of m.
To do so, we fix a value of m, and for each value of K (or equivalently ε or ω):

1. We compute the associated equilibrium point $L_- = (0, 0, 3\varepsilon^{2+m}, 0)$ of the corresponding Hamiltonian system.

2. We compute, using the parameterization method and multiple precision arithmetics, the unstable manifold $W^{\mathrm{u}}(L_-)$ up to the Poincaré section $\widetilde{\Sigma} : x = \pi$. We call (x^u, y^u, q^u, p^u) the corresponding point with $x^u = \pi$.

3. We would proceed similarly with the stable manifold of L_+ and we would compute the intersection point (x^s, y^s, q^s, p^s) with $\widetilde{\Sigma}$. However, due to the symmetry

$$(x, y, q, p, t) \to (2\pi - x, y, q, -p, -t) \tag{64}$$

only the unstable manifold $W^{\mathrm{u}}(L_-)$ needs to be computed since at the Poincaré section we have $x^u = x^s = \pi$, $q^u = q^s$, $p^u = -p^s$ and $y^u = y^s$. We are interested in the splitting between $W^{\mathrm{u}}(L_-)$ and $W^{\mathrm{s}}(L_+)$ at $\widetilde{\Sigma}$, that is, the value

$$\Delta p = p^u - p^s = 2p^u$$

4. We vary the values of K tending to 0 (or ε or ω), and we obtain a set of points $(K_i, \Delta p_i)$, for $i = 1, \dots, N$. In the numerical simulations we have taken decreasing values of K up to $3 \cdot 10^{-8}$. Again order of thousands for the parameterization and multiple precision with thousands of digits are required.

5. We fit the numerical computed values by a formula of type,

$$|\Delta p| \sim \varepsilon^m A |\omega|^r \exp\left(\frac{\omega\pi}{2}\right) \tag{65}$$

or equivalently,

$$\ln|\Delta p| - m \ln \varepsilon - \frac{\omega\pi}{2} \sim \ln A + r \ln|\omega|,$$

where we denote $r = r_{0,m}$ and $A = A_{0,m}$, but we shall keep r and A in the formulas to not overload the notation.

Let us discuss the results obtained. Notice that we want to check two different values: the exponent r, which should be equal to 3, and the constant A, which should be $8\pi/3$ or $\ln A = 2.125591\ldots$. In Fig. 7 we show a first (rough) plot with the points $(\ln|\omega_i|, Y_{\Delta p_i})$ with $Y_{\Delta p_i} := \ln|\Delta p_i| - m \ln \varepsilon_i - \omega_i \pi/2$ (and $\varepsilon_i = (K_i/3)^{1/4}$ and $\omega_i = -1/(3\varepsilon_i^2)$), where we have taken some values of K ranging from 0.005 to $5 \cdot 10^{-8}$. Taking such a big set of values of K for each value of m, we can see how the set of points for each case $m = 1, 2, 3, 4, 5, 6$ overlap on the line $Y = 2.1255 + 3 \ln|\omega|$.

However, formula (65) is an asymptotic formula, so to find out the tendency of r towards 3 and $\ln A$ towards $\ln(8\pi/3) = 2.1255\ldots$ (see the dashed horizontal line in Figs. 8 and 10), we proceed as above, that is, we compute, for each two successive points $(\ln|\omega_i|, Y_{\Delta p_i})$ and $(\ln|\omega_{i+1}|, Y_{\Delta p_{i+1}})$, the segment passing through these two points, with an expression $r_i \ln|\omega| + \ln A_i$. Taking values of K decreasing from 0.005 to $5 \cdot 10^{-8}$, we plot the set of points $(\ln|\omega_i|, r_i)$, $i = 1, \dots, N-1$, in Fig. 8 (left) and $(\ln|\omega_i|, \ln A_i)$, $i = 1, \dots, N-1$, in Fig. 8 (right). These computations are shown for $m = 1, 2, 3, 4, 5, 6$. Some remarks must be mentioned:

(i) It is clear that the value of r tends to 3 for the values of m considered so the exponent 3 in the theoretical Melnikov formula (33) fits with the numerical exponent obtained. Moreover we also observe that for $m = 2, 3, 4, 5, 6$ (say $m \geq 2$) the tendency of r is mainly the same and fast towards the value 3, but for $m = 1$ it takes a bit longer to tend to 3. But in all cases, r tends to 3 when K tends to zero. So we may infer that for any $m \geq 1$, the exponent r is 3.

(ii) Concerning the value of the constant $\ln A$, it is clear that, for $m \geq 2$, $\ln A \to \ln(8\pi/3)$. However, in principle it is not that clear for $m = 1$. Another way to show the tendency of r_i and $\ln A_i$ to 3 and $\ln(8\pi/3) = 2.1255\ldots$ respectively, is based on the computation of the points $(\ln|\omega_i|, |r_i - 3|)$ in Fig. 9 left and the points $(\ln|\omega_i|, |\ln A_i - \ln(8\pi/3)|)$ in Fig. 9 right. We see in the left figure that for $m = 3, 4, 5, 6$ the points *overlap* on the same curve and $|r - 3|$ tends clearly to zero. In particular, for $m = 2$, the curve r crosses the value $r = 3$. See Fig. 8 left (i.e. the points on the curve $(\ln|\omega|, |r - 3|)$ describe a sharp minimum for a value of $\ln|\omega|$ close to 5 and the values of r tend to 3) and we observe the decreasing tendency to zero in Fig. 9 left. We also see a possible decreasing tendency to zero for $m = 1$, but not as fast as the one for $m = 2$ or $m \geq 3$.

Similarly, looking at Fig. 9 right, we observe for $m = 3, 4, 5, 6$ the fast tendency of

$$\left|\ln A - \ln\left(\frac{8\pi}{3}\right)\right|$$

to zero. However for $m = 2$, the curve $|\ln A|$ (see Fig. 8 right) crosses the value $\ln(8\pi/3)$ (it is clearly seen in the sharp minimum for $|\ln A - \ln(8\pi/3)|$ in Fig. 9 right), has a local maximum and goes on decreasing tending to $\ln(8\pi/3)$ (we observe a slower tendency to zero in Fig. 9 right). Similarly we could expect this to happen for $m = 1$. Actually we see the crossing value $\ln(8\pi/3)$, and (almost) the maximum. However we cannot observe the decreasing tendency to $\ln(8\pi/3)$ as expected.

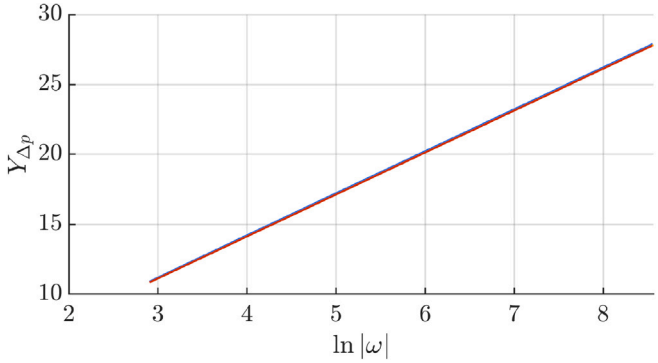

Fig. 7. Points $(\ln|\omega_i|, Y_{\Delta p_i})$ for $m = 1, 2, 3, 4, 5, 6$. Notice they *overlap* on a line.

To study more carefully the case $m = 1$, the previous computation naturally leads to explore the behavior of r and $\ln A$ for intermediate values of m between 1 and 2, to see the continuous evolution. This has been done for $m = 1.1, 1.2, 1.3, \dots, 1.9$ and we show the results in Fig. 10 left for r and right for $\ln A$. We notice the continuous evolution of the curves for the intermediate different values of m. In particular, on the left plot we see the tendency of r to 3 for any value of m. On the right plot we see the maximum in each curve $\ln A$ for $m = 1.1, \dots, 1.9$ and the asymptotic tendency to $2.1255\dots$, as $\ln|\omega|$ increases, however for $m = 1$ we see the maximum but not the expected decreasing tendency to $2.1255\dots$. To do so, we should consider smaller values of K. But this becomes numerically unfeasible (to compute the value of Δp for $K = 5 \cdot 10^{-8}$ we need thousands of digits and an order of thousands for the parameterization of the manifold, so smaller values of K become prohibitive).

6. A double check concerning the value of A is related to the extrapolation procedure done in Section 3.3. More precisely, for every value of $m \geq 1$ fixed, we apply (finite) extrapolation steps to the first fit formula:

$$\frac{|\Delta p||\omega|^{-r} \exp\left(-\frac{\omega\pi}{2}\right)}{\varepsilon^m} \sim A + A_2\varepsilon^2 + A_4\varepsilon^4 + \cdots$$

or to the second fit formula

$$\frac{|\Delta p||\omega|^{-r} \exp\left(-\frac{\omega\pi}{2}\right)}{\varepsilon^m\left(1 - \frac{2}{\omega^2}\right)} \sim \tilde{A} + \tilde{A}_2\varepsilon^2 + \tilde{A}_4\varepsilon^4 + \cdots$$

both formulas with $r = 3$. We also want to compare both formulas and to check if the second one somewhat improves the first one.

Our simulations show that, as m increases, the number of digits obtained for the value of $A_{0,m} = 8\pi/3$ also increases when taking the second fit formula instead of the first one. For example, for $m = 6$ we obtain, respectively, 6, 10 digits when taking a first step and a second step of extrapolation using the first fit formula, whereas we obtain 20, 20 digits with two successive steps of extrapolation applied to the second fit formula. However, as m decreases, for example $m = 1$, neither the first nor the second fit formula, even using extrapolation, are able to provide good digits of $A_{0,1}$. As mentioned above, we should need smaller values of K, which is not feasible.

So, from the numerical simulations, we can conclude that for the Toy CP problem with $a = 0$, Hamiltonian (63),

(i) Formula

$$|\Delta p| \sim \varepsilon^m A|\omega|^r \exp\left(\frac{\omega\pi}{2}\right) \tag{66}$$

with $r = r_{0,m} = 3$ and $A = A_{0,m} = 8\pi/3$, provides a good fit formula for the splitting Δp, and

(ii) The Melnikov formula predicts the splitting for any $m > 1$ both in $r_{0,m}$ and $A_{0,m}$. However, for $m = 1$, while the tendency of $r_{0,1}$ to 3 is clear, we cannot conjecture this tendency to happen for $\ln A_{0,1}$ to $\ln(8\pi/3) = 2.1255\dots$ since the numerical results are not conclusive enough.

4.3. Other strategies/models to fit the numerical computation of Δp for the CP problem

Recall that our purpose is to find a simplified model that *mimics* the splitting Δp of the CP problem in resonant coordinates. And we have just shown that the standard perturbed pendulum, $H_{0,1} = H_0 + \varepsilon H_1$, is not good enough. So we want to find out another simple model that *does* describe the splitting of the CP problem. A natural procedure is to take the second order approximation

$$H = H_0 + \varepsilon H_1 + \varepsilon^2 H_2$$

see (57), and consider different truncated Hamiltonians adding to $H_0 + \varepsilon H_1$ different terms of $\varepsilon^2 H_2$. For each selected Hamiltonian, we, first, take a value of K and we compute the splitting Δp (obtained from the intersection of the unstable manifold of the corresponding equilibrium point and the section $x = \pi$, $y > 0$). Second, we repeat the procedure for different decreasing values of K and, third, we fit Δp by an expression of the type

$$|\Delta p| \sim \varepsilon A|\omega|^r \exp\left(\frac{\omega\pi}{2}\right)$$

and we want to know which terms of the Hamiltonian are relevant that give rise to a value of r equal to the one obtained for the CP problem, that is $r_{\text{CPR}} = 2.111\dots = 19/9$. We have done the numerical computations considering different truncated Hamiltonians taking different terms of H_2. We have used just quadruple precision and decreasing values of K ranging from 0.001 to $5 \cdot 10^{-5}$ to have a first insight. From these numerical

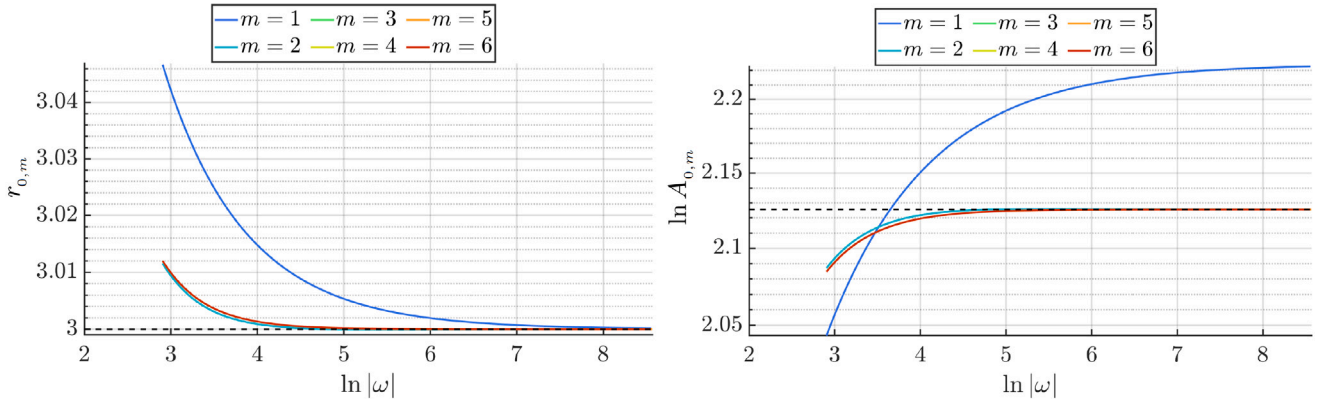

Fig. 8. The perturbed standard pendulum. Points $\left(\ln|\omega|, r_{0,m}\right)$ (left), and $\left(\ln|\omega|, \ln A_{0,m}\right)$ (right) obtained for $m = 1, \ldots, 6$. The dashed line (on the right figure) corresponds to the value $\ln(8\pi/3) = 2.1255\ldots$.

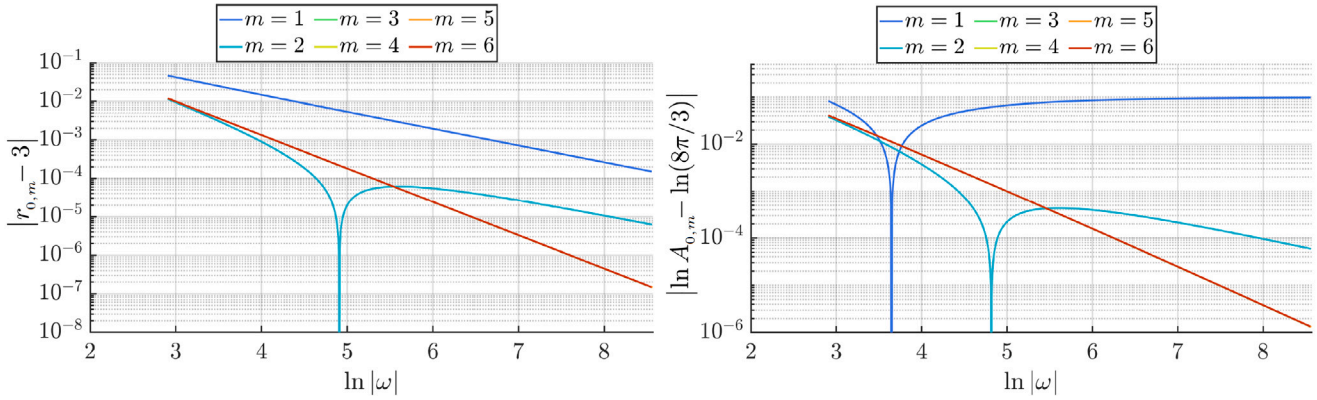

Fig. 9. The toy CP problem corresponding to $a = 0$. Points $\left(\ln|\omega|, \left|r_{0,m} - 3\right|\right)$ (left), and points $\left(\ln|\omega|, \left|\ln A_{0,m} - \ln(8\pi/3)\right|\right)$ (right) are obtained for $m = 1, \ldots, 6$.

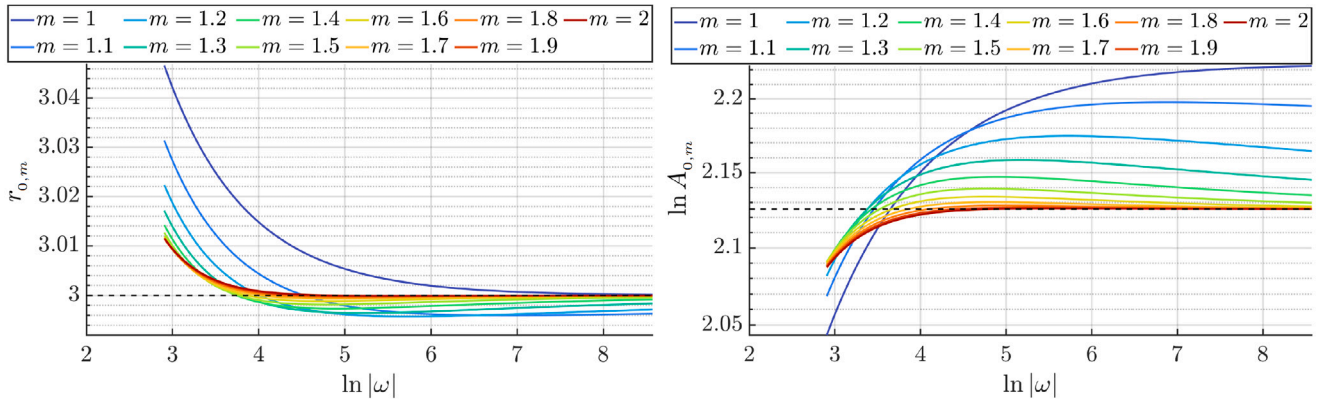

Fig. 10. The Toy CP problem with $a = 0$. Points $\left(\ln|\omega|, r_{0,m}\right)$ left, and $\left(\ln|\omega|, \ln A_{0,m}\right)$ right obtained for $m = 1, 1.1, \ldots, 2$. The dashed line (on the right figure) corresponds to the value $\ln(8\pi/3) = 2.1255\ldots$.

simulations we can conclude that the simplest model that reproduces the value of $r_{\text{CPR}} = 2.111\ldots$ for the fitting splitting formula is the Hamiltonian provided by $H_0 + \varepsilon H_1 - (2/3)\varepsilon^2 y^3$, that is, only the term $-(2/3)\varepsilon^2 y^3$ in H_2 is responsible for changing the exponent $r_{0,1} = 3$ (obtained from the standard perturbed pendulum) to $r_{\text{CPR}} = 2.1111\ldots$.

So, in next Section we will consider this precise Hamiltonian and we will use multiple precision computations in order to show that we really obtain the value $r_{\text{CPR}} = 2.1111\ldots = 19/9$.

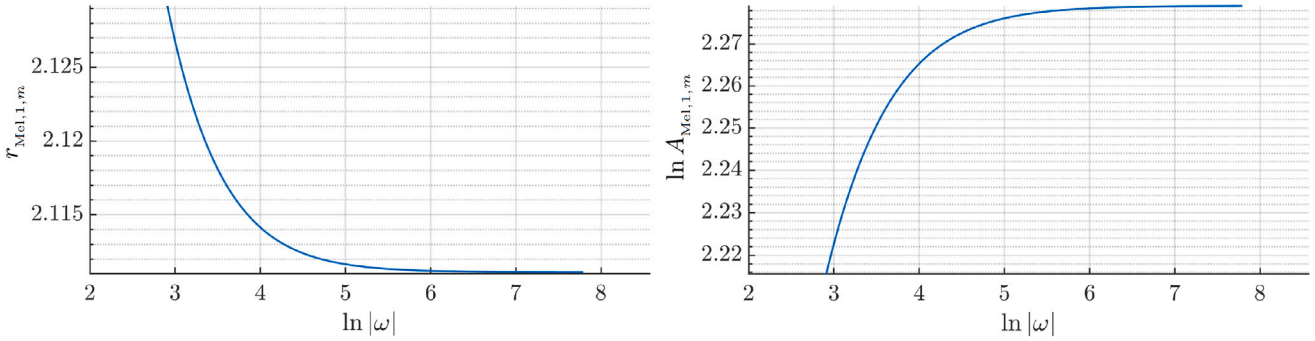

Fig. 11. Curves $\left(\ln|\omega|, r_{\mathrm{Mel},1,m}\right)$ and $\left(\ln|\omega|, \ln A_{\mathrm{Mel},1,m}\right)$ obtained from the computation of the Melnikov integral.

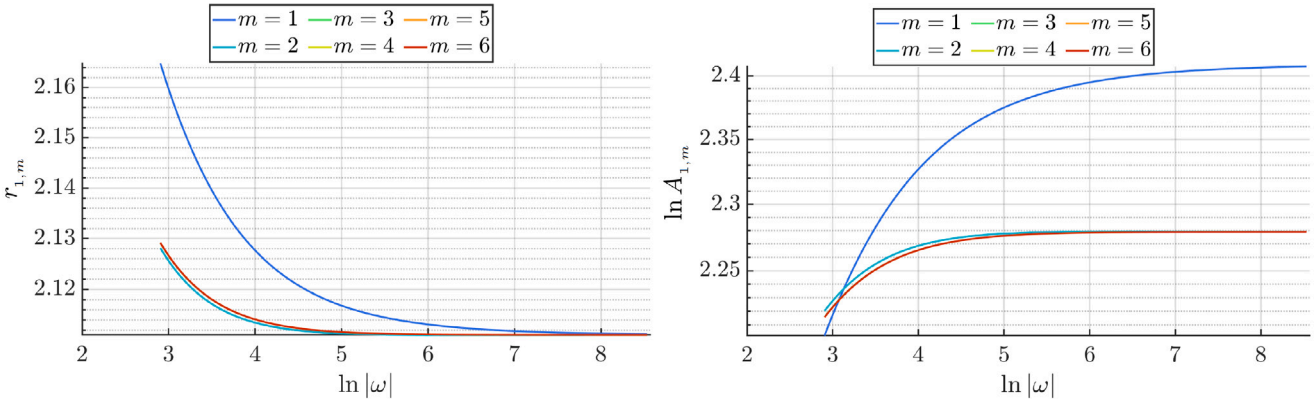

Fig. 12. The Toy CP problem with $a = 1$. Points $\left(\ln|\omega|, r_{1,m}\right)$ (left), and $\left(\ln|\omega|, \ln A_{1,m}\right)$ (right) obtained for $m = 1, \ldots, 6$.

5. The Toy CP problem with $a = 1$

The previous discussion motivates to analyze the new Hamiltonian adding the term $(-2/3)\varepsilon^2 y^3$ to the integrable part H_0 giving rise to a new integrable part,

$$H_0(x, y, q, p) - \frac{2}{3}\varepsilon^2 y^3, \tag{67}$$

which we will call *amended pendulum*, plus the perturbation $\varepsilon H_1(x, y, q, p)$, called from now on the *perturbed amended pendulum*. Or, more generally, we consider the Toy CP problem with $a = 1$ and $m \geq 1$, i.e.,

$$H_{1,m}(x, y, q, p) = H_0(x, y, q, p) - \frac{2}{3}\varepsilon^2 y^3 + \varepsilon^m H_1(x, y, q, p).$$

In this Section we will carry out two kind of computations:

(i) the computation of the Melnikov integral for Δp (see formulas (31) and (34)). In this case, however, we cannot compute the Melnikow integral for the amended pendulum analytically (as we did for the standard pendulum) since no parameterization of the homoclinic loop (the separatrices) for the integrable part (67) is available. So the Melnikov integral will be computed numerically. This will be done in Section 5.1.

(ii) The computation of the splitting Δp (of the unstable and stable manifolds of the corresponding equilibrium points) at the Poincaré section $\widetilde{\Sigma}$. This will be done in Section 5.2.

(iii) Finally, we will discuss Melnikov prediction of the splitting, on the one hand for the Toy CP problem in Section 5.2, and on the other hand for the CP problem in Section 5.3.

5.1. Numerical computation of the Melnikov formula using the amended pendulum

Recall formula (27) that provides the linear approximation of the splitting $\Delta v_1(t) = (\Delta q_1(t), \Delta p_1(t))$. We are interested in the splitting at $t = 0$, so we use formula (34) for $\Delta v_1(0) = (\Delta q_1(0), \Delta p_1(0))$. In particular, for $H_1(x, y, q, p)$ in (29) we obtain

$$\Delta q_1(0) = 0, \qquad \Delta p_1(0) = -\frac{1}{2}\int_{-\infty}^{\infty} (\cos(2x(t) + \omega t) - \cos\omega t)\, \mathrm{d}t,$$

where $(x(t), y(t))$ defines the separatrix of $\breve{H}_0$ and the right hand side term is precisely the *Melnikov integral*.

So an strategy to compute the Melnikov integral consists of integrating the system of ODE

$$\begin{cases} \dot{x} = y - 2\varepsilon^2 y^2, \\ \dot{y} = \sin x, \\ \dot{z} = \cos(2x + \omega t) - \cos \omega t, \end{cases} \tag{68}$$

and more particularly the Melnikov integral

$$\frac{1}{2}\int_{-\infty}^{\infty} [\cos(2x + \omega t) - \cos \omega t]\, \mathrm{d}t = \int_{-\infty}^{0} [\cos(2x + \omega t) - \cos \omega t]\, \mathrm{d}t$$

due to the symmetry (64). So if $z(t) = \int_{-\infty}^{t} \dot{z}(u)\mathrm{d}u$ we want to compute the value $z(0)$.

We proceed with the following steps:

Step 1: Applying the parameterization method (see Appendix B) we obtain a local approximation of the unstable manifold (separatrix), $W^u(0)$, associated with the equilibrium point $(0, 0)$ of the system

$$\begin{cases} \dot{x} = y - 2\varepsilon^2 y^2 \\ \dot{y} = \sin x \end{cases} \tag{69}$$

that is, we have a (high order expansion of a) parameterization of the separatrix given by:

$$\sum_{k=1}^{N} \boldsymbol{w}_k s^k + O(s^{N+1}) \tag{70}$$

Step 2: We compute a suitable value $\hat{s}$ small enough such that the error in this approximation is less than some given tolerance.

Step 3: We follow numerically the solution (the separatrix) of system (69) from the point

$$(x, y) = \sum_{k=1}^{N} \boldsymbol{w}_k \hat{s}^k$$

up to the section $\widetilde{\Sigma}$ $(x = \pi)$ and compute the necessary time, T, to reach $\widetilde{\Sigma}$.

Step 4: We define $s_0 = \dfrac{\hat{s}}{e^{-T}}$.

Step 5: We compute the integral of the function $z(t)$ from $-\infty$ to $-T$. To do so, we notice that from the Hamiltonian $\check{H}_0$ in (67) and taking into account the value $H = h = 0$ at $(0, 0)$,

$$\cos x = 1 - \frac{y^2}{2} + \frac{2}{3}\varepsilon^2 y^3$$

and we have

$$\dot{z} = \cos(2x + \omega t) - \cos \omega t = -2\dot{y}^2 \cos \omega t + \dot{y}\left(-2 + y^2 - \frac{4}{3}\varepsilon^2 y^3\right) \sin \omega t. \tag{71}$$

We notice that from (70) we have, in particular, the expansion of $y(t)$:

$$y(t) = y_1 s_0 e^t + y_2 s_0^2 e^{2t} + y_3 s_0^3 e^{3t} + \cdots = y_1 s + y_2 s^2 + y_3 s^3 + \cdots$$

Thus, the expression of $\dot{z}$ in (71) becomes an expansion in s (or equivalently in $s_0 e^t$) together with the terms $\sin(\omega t)$ and $\cos(\omega t)$. We just need to integrate $\dot{z}(t)$ from $-\infty$ to $-T$. Let us provide a formula for the appearing terms in the integral:

$$\int_{-\infty}^{-T} a_k s^k \cos \omega t\, \mathrm{d}t = a_k \hat{s}^k \frac{k \cos(-\omega T) + \omega \sin(-\omega T)}{k^2 + \omega^2},$$
$$\int_{-\infty}^{-T} a_k s^k \sin \omega t\, \mathrm{d}t = a_k \hat{s}^k \frac{k \sin(-\omega T) - \omega \cos(-\omega T)}{k^2 + \omega^2}.$$

Step 6: Once we get the value $z(-T) = \int_{-\infty}^{-T} \dot{z}(t)\, \mathrm{d}t$ we integrate numerically system (68) from $-T$ to 0, and we obtain $z(0)$.

Taking different decreasing values of K from $K = 0.001$ to $K = 5.7 \cdot 10^{-8}$, we fit the output values for the Melnikov integral by the formula

$$z(0) \sim A|\omega|^r \exp\left(\frac{\omega\pi}{2}\right) \tag{72}$$

or

$$\ln z(0) - \frac{\omega\pi}{2} \sim r \ln|\omega| + \ln A,$$

and we obtain (see Fig. 11)

$$r = r_{\mathrm{Mel},1,m} = 2.111\ldots = \frac{19}{9}, \qquad \ln A = \ln A_{\mathrm{Mel},1,m} = 2.279\ldots \tag{73}$$

We remark the good coincidence of the value of $r_{\mathrm{Mel},1,m}$ with that obtained for the CP problem in resonant coordinates, r_{CPR}.

Concerning the value of $\ln A_{\mathrm{Mel},1,m}$, there is not such coincidence with that obtained for the CP problem in resonant coordinates, $\ln A_{\mathrm{CPR}}$.

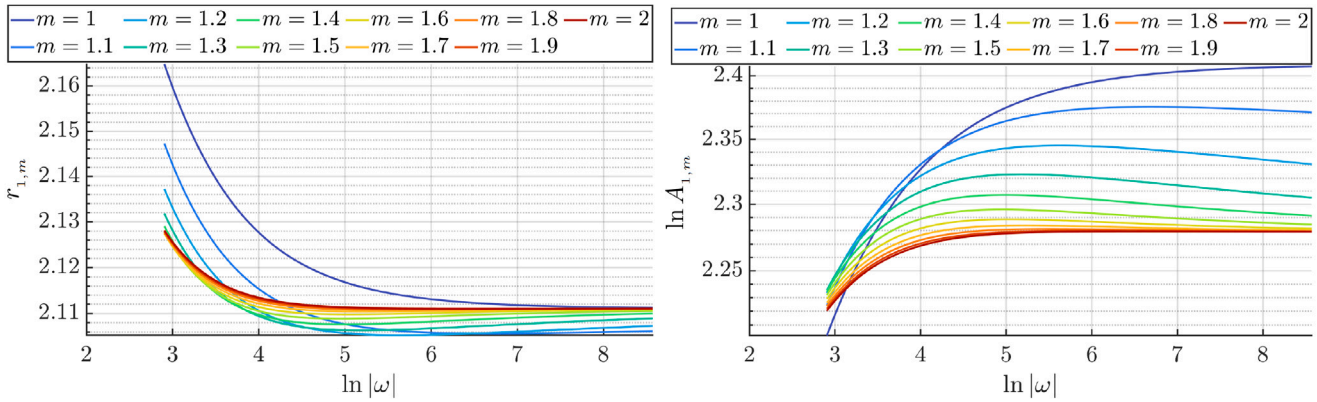

Fig. 13. The Toy CP problem with $a = 1$. Points $\left(\ln|\omega|, r_{1,m}\right)$ (left), and $\left(\ln|\omega|, \ln A_{1,m}\right)$ (right) obtained for $m = 1, 1.1, 1.2, \ldots, 2$.

5.2. Straight numerical computation of the splitting Δp

Similarly as we proceeded for the standard perturbed pendulum, we consider the Toy CP problem with $a = 1$, that is,

$$H_{1,m}(x, y, q, p) = H_0(x, y, q, p) - \frac{2}{3}\varepsilon^2 y^3 + \varepsilon^m H_1(x, y, q, p).$$

We fix a value of $m \geq 1$, we take different values of K (decreasing up to $3 \cdot 10^{-8}$), and for each K given we compute the unstable manifold of the equilibrium point $L_- = (0, 0, 3\varepsilon^{2+m}, 0)$ intersection with $\widetilde{\Sigma}$ and we focus on the splitting $\Delta p = 2p^u$, which we want to fit by

$$|\Delta p| \sim \varepsilon^m A|\omega|^r \exp\left(\frac{\omega\pi}{2}\right), \tag{74}$$

or equivalently,

$$\ln|\Delta p| - m\ln\varepsilon - \frac{\omega\pi}{2} \sim r\ln|\omega| + \ln A. \tag{75}$$

In this case, unlike the perturbed standard pendulum problem, we do not know neither the value of r, denoted as $r = r_{1,m}$, nor the value of $\ln A$ denoted as $\ln A = \ln A_{1,m}$ in formula (75).

We plot in Fig. 12 left the obtained points $(\ln|\omega_i|, r_i)$ (similarly as we did above, that is, taking a segment between two successive points $(\ln|\omega_i|, Y_{\Delta p_i})$, $(\ln|\omega_{i+1}|, Y_{\Delta p_{i+1}})$, with $Y_{\Delta p} := \ln|\Delta p| - m\ln\varepsilon - \omega\pi/2$). We observe the tendency of r towards the value $2.111115\ldots$, which coincides with the value of $r_{\mathrm{Mel},1,m}$ obtained from the Melnikov integral.

Regarding the value of $\ln A$, it is apparently clear that for $m \geq 2$, $\ln A$ tends to $2.279\ldots$, which coincides with the value of $\ln A$ obtained from the Melnikov integral. However it is not that clear for $m = 1$. Analogously as we did for the standard perturbed pendulum, we now explore the intermediate values $m = 1.1, 1.2, 1.3, 1.4, \ldots, 1.9$ between $m = 1$ and $m = 2$. The results are shown in Fig. 13 left —for r— and right —for $\ln A$—. The continuous evolution is clear. So we would expect, for $m = 1$, a tendency of $\ln A$ to $2.279\ldots$. But again, as in the perturbed standard pendulum case, for $m = 1$, we need smaller values of K (which turns out to be prohibitive from a numerical point of view).

So, from the numerical computations done, we can conclude that for the Toy CP problem with $a = 1$,

(i) the formula (75) provides a good fitting for Δp with

$$r_{1,m} = 2.111\ldots = 19/9, \qquad A_{1,m} = 2.279\ldots \qquad \text{for } m > 1, \tag{76}$$

and

$$r_{1,1} = 2.111\ldots = 19/9, \qquad A_{1,1} = ? \qquad \text{for } m = 1, \tag{77}$$

(ii) The Melnikov integral *does* predict the value of the exponent $r_{\mathrm{Mel},1,m} = r_{1,m} = 19/9$ for $m \geq 1$ and the value of $\ln A_{\mathrm{Mel},1,m} = \ln A_{1,m} = 2.279\ldots$ for $m > 1$, but the numerical results are not conclusive for $m = 1$.

5.3. Agreement between the real CP problem and the Toy CP problem with $a = m = 1$

(i) Concerning the computation of the splitting Δp (from the unstable/stable manifolds at the intersection with $x = \pi$, $y > 0$), we now consider two different problems: the original CP problem in resonant coordinates and the perturbed amended pendulum with $m = 1$, that is, the Toy CP problem with $a = m = 1$. We want to compare the respective values of r_{CPR} and $r_{1,1}$ in the corresponding fit formulas (49) and (74).

More precisely, concerning the values of r_{CPR} and $r_{1,1}$, we want to compare two curves, the numerical obtained curve, $\left(\ln|\omega|, r_{\mathrm{CPR}}\right)$, for the splitting in resonant coordinates of the original CP Hamiltonian, and the numerical obtained curve, $\left(\ln|\omega|, r_{1,1}\right)$, for the splitting of the perturbed amended pendulum Hamiltonian (with $m = 1$). In Fig. 14 left we plot the curve $\left(\ln|\omega|, \left|r_{1,1} - r_{\mathrm{CPR}}\right|\right)$ to find out the differences between both values. We remark the very good agreement of both values as far as K decreases (or equivalently $\ln|\omega|$ increases).

Concerning the values of $\ln A_{\mathrm{CPR}}$ and $\ln A_{1,1}$ in formulas (49) and (74), it seems that $\ln A_{\mathrm{CPR}} = \ln A_{1,1} + \ln\left(2\sqrt{2}\right)$. Right now we do not foresee any specific reason for this $\ln 2\sqrt{2}$ term.

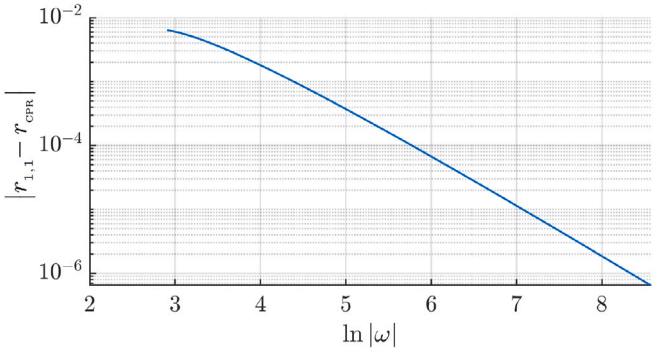

Fig. 14. Curve $\left(\ln|\omega|, \left|r_{1,1} - r_{CPR}\right|\right)$ when computing the straight splitting from the CP problem and the perturbed amended pendulum (with $m = 1$). See the text for details.

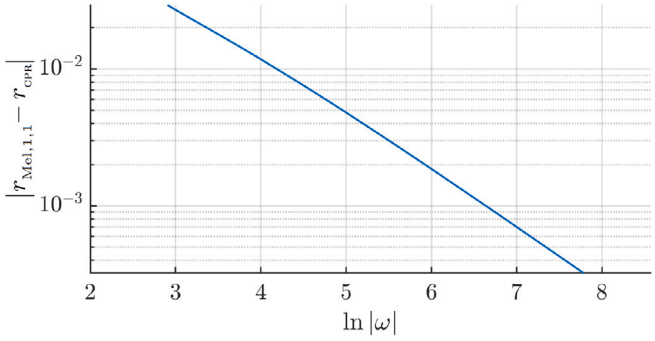

Fig. 15. Curve $\left(\ln|\omega|, \left|r_{Mel,1,1} - r_{CPR}\right|\right)$ when computing the straight splitting from the CP problem and the splitting using the Melnikov integral of the perturbed amended pendulum (with $m = 1$). See the text for details.

Table 3
Corresponding values of r and A in the fitting formula (78) of $|\Delta\dot{\chi}|$ (first row) and $|\Delta p|$ (remaining rows). (C) stands for a numerical conjectured value.

Hamiltonian	j	r	$\ln A$	Section	Formula
H_{CP}, $\|\Delta\dot{\chi}\|$	1	$r_{CP} = 29/18$ (C)	$\ln A_{CP} = 2.77603950$ (C)	3.2	(48)
H_{CPR}, $\|\Delta p\|$	1	$r_{CPR} = r_{CP} + 1/2$	$\ln A_{CPR} = \ln A_{CP} + \ln\sqrt{3} = 3.325345645$	3.3	(56)
Toy CP $H_{0,m}$, $m > 1$, $\|\Delta p\|$	m	3	$\ln A_{0,m} = \ln(8\pi/3)$	4.2	(66)
Toy CP $H_{0,1}$, $\|\Delta p\|$	1	3	$\ln A_{0,1} = ?$	4.2	(66)
Toy CP $H_{1,m}$, $m > 1$, $\|\Delta p\|$	m	19/9	$\ln A_{1,m} = 2.279...$	5.2	(76)
Toy CP $H_{1,1}$, $\|\Delta p\|$	1	19/9	$\ln A_{1,1} = ?$	5.3	(77)

So we can conclude that the perturbed amended pendulum is a simplified model that already describes the splitting of the CP problem, as far as the asymptotic behavior (when K tends to zero) is concerned.

(ii) Finally, how does the Melnikov integral (taking into account the CP problem with $a = m = 1$) predict the splitting for the CP problem in resonant coordinates? That is, we want to compare the fit formulas for Δp (of the CP problem, that is (49)) and for the Melnikov integral (of the perturbed amended pendulum problem with $m = 1$, that is (72)), more precisely, the values of the exponents r_{CPR} and $r_{Mel,1,1}$ and the values of A_{CPR} and $A_{Mel,1,1}$.

In Fig. 15 we observe the difference $\left|r_{Mel,1,1} - r_{CPR}\right|$ tending to zero. So we can conclude that the fitting asymptotic formula obtained for the Melnikov integral provides the same limit value of the exponent $r_{CPR} = r_{Mel,1,1} = 2.111\ldots = 19/9$. However, concerning the constant A, the Melnikov integral estimate does not seem to fit since we obtain the relation $\ln A_{CPR} = \ln A_{Mel,1,1} + \ln\left(2\sqrt{2}\right)$.

6. Summary of results

We have mainly discussed the asymptotic formulas to fit the splitting of 1D-invariant manifolds of equilibrium points in different models. The expression

$$\varepsilon^j A|\omega|^r \exp\left(\frac{\omega\pi}{2}\right) \tag{78}$$

turns out to be a good fitting formula.

In Tables 3 and 4 we provide a summary of the different values of A and r in the corresponding expressions. (C) stands for a numerical conjectured value.

Table 4
Corresponding values of r and A in the fitting formula (78) of the Melnikov integral for $|\Delta p|$.

Hamiltonian	r_{Mel}	$\ln A_{\text{Mel}}$	Section	Formula
Toy CP $H_{0,m}$, $m \geq 1$	3	$\ln(8\pi/3)$	4.1	(62)
Toy CP $H_{1,m}$, $m \geq 1$	19/9	2.279... (C)	5.1	(73)

Concerning the computation of the splitting $\Delta\dot{x}$ and Δp and the associated fitting formula:

(i) The value of the exponent r is numerically approximated for the CP problem (in synodical coordinates and Poincaré resonant ones), satisfying the relation $r_{\text{CPR}} = r_{\text{CP}} + 1/2$ and for the Toy CP model (both cases $a = 0$ and $a = 1$).

(ii) The value of A is numerically approximated for the Toy CP problem (both cases $a = 0$ and $a = 1$) and $m > 1$.

(iii) The value of A for the Toy CP model with $m = 1$ is not reliable enough. Actually a higher number of digits should be needed which is unfeasible at present from a numerical point of view.

Concerning the computation of the Melnikov integral:

(i) It can be computed analytically only for the Toy CP model with $a = 0$, where the values of the exponent r and of the constant A are analytically obtained (see (62)).

(ii) For the Toy CP problem with $a = 1$, the value of the exponent r is numerically approximated whereas the value of A is not reliable enough. Again, a higher precision should be needed.

Concerning the good agreement between the different models:

(i) The relation $r_{\text{CPR}} = r_{\text{CP}} + 1/2$ is analytically justified.

(ii) The values for the exponent r taken from Tables 3 and 4 coincide, that is,

$$r_{\text{CPR}} = r_{1,1} = r_{\text{Mel},1,1} = 19/9,$$

so the Toy CP problem is a simpler model that provides the asymptotic behavior of the splitting for the CP problem, as far as the value of r is taken into account. For the value of A, a modified Toy CP problem appears to be required.

We finally recall that the numerical results have been obtained using high precision computations (dealing with up to five thousand digits).

Remark. In Section 4, where we considered the perturbed standard pendulum, we discussed the known results (in the literature) compared with the ones obtained in this paper. However, for the Toy CP problem we are not aware of any published results.

CRediT authorship contribution statement

Amadeu Delshams: Writing – review & editing, Writing – original draft, Software, Methodology, Investigation, Funding acquisition, Formal analysis, Conceptualization. **Mercè Ollé:** Writing – review & editing, Writing – original draft, Software, Methodology, Investigation, Funding acquisition, Formal analysis, Conceptualization. **Juan Ramon Pacha:** Writing – review & editing, Writing – original draft, Software, Methodology, Investigation, Funding acquisition, Formal analysis, Conceptualization. **Óscar Rodríguez:** Writing – review & editing, Writing – original draft, Software, Methodology, Investigation, Funding acquisition, Formal analysis, Conceptualization.

Declaration of competing interest

The authors declare that they have no known competing financial interests or personal relationships that could have appeared to influence the work reported in this paper.

Acknowledgments

This work is supported by the Spanish State Research Agency, Spain, through the Severo Ochoa and María de Maeztu Program for Centers and Units of Excellence in R&D (CEX2020-001084-M). The authors were also supported by the Spanish grant PID2021-123968NB-I00 (MICIU/AEI/10.13039/
501100011033/FEDER/UE).

Appendix A. Computation of $\mathcal{A}^{\pm}(\omega)$

In this Appendix we explain how to derive the formula (35) that gives $\mathcal{A}^{\pm}(\omega)$ when $x_0(t) = x_0^{\pm}(t)$ is that of the standard pendulum given in (21). In particular we take $x_0(t) = x_0^{+}(t)$, so we consider the external branch ($y_0(t) = y_0^{+}(t) > 0$). For the internal branch ($y_0(t) = y_0^{-}(t) < 0$) the process that leads to $\mathcal{A}^{-}(\omega)$ can be carried out in a similar way, so we will not give the details here.

Let $(x_0^{\pm}(s), y^{\pm}(s))$ be the parameterization of the separatrices of the standard pendulum given in (21), and let $(x(s), y(s))$ denote specifically the external one, i.e.,

$$x_0(s) = x_0^{+}(s) = 4\arctan(\mathrm{e}^{s}), \qquad y_0(s) = \dot{x}_0(s) = y_0^{+}(s) = \frac{2}{\cosh s}.$$

Following [35] we define

$$\mathcal{J}(a,b) := \int_{-\infty}^{\infty} \mathrm{e}^{\mathrm{i}as}\mathrm{e}^{\mathrm{i}b\frac{x_0(s)-\pi}{2}} y_0(s)\,\mathrm{d}s, \tag{79}$$

that, as it is pointed out there, is real whenever a and b are real. With the above definition, integrating by parts the complex expression (30) of the real formula (35), it follows at once that

$$\mathcal{A}(\omega) = \int_{-\infty}^{\infty} \mathrm{e}^{\mathrm{i}\omega s}\left(1 - \mathrm{e}^{2\mathrm{i}x_0(s)}\right) \mathrm{d}s = \left[\mathcal{Q}_\omega(r)\right]_{-\infty}^{\infty} + \frac{2}{\omega}\mathcal{J}(\omega, 4), \tag{80}$$

where

$$\mathcal{Q}_\omega(r) = \frac{\mathrm{e}^{\mathrm{i}\omega r}}{\mathrm{i}\omega}\left(1 - \mathrm{e}^{\mathrm{i}4\frac{x_0(r)-\pi}{2}}\right) = \frac{\mathrm{e}^{\mathrm{i}\omega r}}{\mathrm{i}\omega}\left[1 - \left(\frac{1 + \mathrm{i}\sinh r}{\cosh r}\right)^4\right],$$

so the "integrated" part at the rhs of (80) vanishes, since

$$\left[\mathcal{Q}_\omega(r)\right]_{-\infty}^{\infty} = \lim_{r\to\infty} \mathcal{Q}_\omega(r) - \lim_{r\to-\infty} \mathcal{Q}_\omega(r)$$

and clearly $\mathcal{Q}_\omega(r) \to 0$ as $r \to \pm\infty$. Hence, from (80), $\mathcal{A}(\omega) = 2\mathcal{J}(\omega, 4)/\omega$ and finally, we can use the formulas given in [35], Section 3.2, to compute (79) for $a = \omega$, $b = 4$. Thus, after some algebra, it is seen that

$$\mathcal{A}(\omega) = \frac{2}{\omega}\mathcal{J}(\omega, 4) = \frac{4}{3}\omega^3\left(1 - \frac{2}{\omega^2}\right)\left[\frac{1}{\cosh\left(\frac{\pi\omega}{2}\right)} - \frac{1}{\sinh\left(\frac{\pi\omega}{2}\right)}\right] = \frac{16\pi}{3}\omega^3\left(1 - \frac{2}{\omega^2}\right)\frac{\mathrm{e}^{\pi\omega/2}}{1 - \mathrm{e}^{2\pi\omega}},$$

which is Eq. (35) corresponding to $c^{\pm} = 1$.

Appendix B. Parameterization method

Let us assume that z^* is a fixed point of the system $\dot{z} = F(z)$ with $F : \mathbb{R}^n \to \mathbb{R}^n$ regular enough. A simple strategy to compute an invariant manifold (W) associated with the point z^* involves first calculating the tangent linear space of W at z^*, i.e., $T_{z^*}W$. Points on $T_{z^*}W$ that are sufficiently close to z^* can then be used as initial conditions for approximating W.

In this section, we focus specifically on computing the unstable manifold $W^u(z^*)$, which we assume to be one-dimensional. The computation for $W^s(z^*)$ is analogous. Thus, we consider that $DF(z^*)$ has a unique eigenvalue $\lambda > 0$ with geometric multiplicity 1, and we denote its associated eigenvector by v.

A common strategy to compute a numerical approximation of the unstable invariant manifold of z^*, $W^u(z^*)$, is to take initial points $z^* + sv$ and $z^* - sv$ with $s > 0$ sufficiently small, and integrate forward in time. This approach provides a straightforward method to approximate the desired invariant manifold. However, this strategy does not always produce sufficiently accurate results. In such cases, the parameterization method [39–41] can be used to obtain very efficient approximations of these invariant manifolds to any desired order.

To find this approximation, we need to determine a parameterization $z = W(s)$, with $s \in \mathbb{R}$, of the invariant manifold $W^u(z^*)$ such that $W(0) = z^*$. This way, the internal dynamics of the manifold are described by the field $\dot{s} = f(s)$ with $f(0) = 0$, and the invariance equation is given by:

$$F(W(s)) = DW(s)f(s). \tag{81}$$

To solve (81), we will find expansions for W and f. in particular, we consider:

$$\begin{cases} W(s) = z^* + \sum_{k\geq 1} W_k(s) = z^* + \sum_{k\geq 1} w_k s^k, & \text{with } w_1 = v, \\ f(s) = \sum_{k\geq 1} f_k(s) = \sum_{k\geq 1} f_k s^k, & \text{with } f_1 = \lambda, \end{cases}$$

where $w_k \in \mathbb{R}^n$ and $f_k \in \mathbb{R}$ $\forall k$.

The goal is to compute w_k and f_k for $k > 1$ once the preceding terms $W_{<k}(s)$ and $f_{<k}(s)$ are known (i.e., given $w_1, \dots, w_{k-1}$ and $f_1, \dots, f_{k-1}$).

First, let us observe that we know the expression on the left side of the invariance equation (81) up to order $k - 1$, i.e.,

$$\left[F(W_{<k}(s))\right]_{<k} = \left[F\left(z^* + \sum_{i=1}^{k-1} W_i(s)\right)\right]_{<k}.$$

Thus, we will first calculate the homogeneous terms of degree k for the composition $F(W_k(s))$ and the matrix product $DW_{<k}(s)f_{<k}(s)$, which we denote by:

$$\left[F(W_{<k}(s))\right]_k = \left[F\left(z^* + \sum_{i=1}^{k-1} W_i(s)\right)\right]_k,$$

$$\left[DW_{<k}(s)f_{<k}(s)\right]_k = \sum_{i=2}^{k-1} DW_i(s)f_{k+1-i}(s) = s^k \sum_{i=2}^{k-1} i\, w_i f_{k+1-i}.$$

In this way, we have:

$$\begin{aligned} \left[F(W_{\leq k}(s))\right]_k &= \left[F(W_{<k}(s))\right]_k + DF(z^*)W_k(s) \\ &= \left[F(W_{<k}(s))\right]_k + DF(z^*)w_k s^k, \end{aligned}$$

and

$$\begin{aligned} \left[DW_{\leq k}(s)f_{\leq k}(s)\right]_k &= \left[DW_{<k}(s)f_{<k}(s)\right]_k + DW_k(s)f_1(s) + DW_1(s)f_k(s) \\ &= \left[\sum_{i=2}^{k-1}\left(i\, w_i f_{k+1-i}\right) + \lambda k w_k + v f_k\right] s^k. \end{aligned}$$

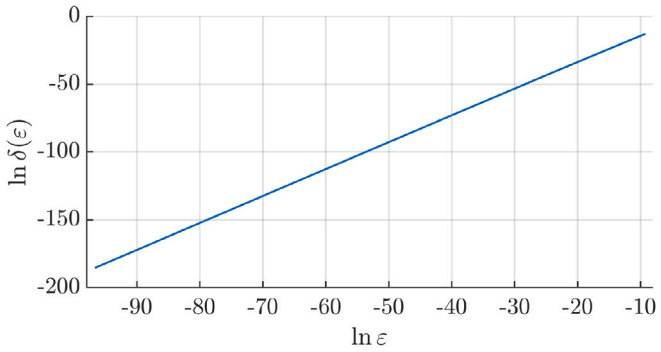

Fig. 16. Points $(\ln\varepsilon, \ln\delta(\varepsilon))$ obtained from the numerical computations.

This leads to the cohomological equation of order k for w_k and f_k:

$$\left[\left(DF(z^*) - \lambda k\, Id\right) w_k - v f_k\right] s^k = -E_k(s), \tag{82}$$

where Id denotes the identity matrix and $E_k(s) = \left[F(W_{<k}(s))\right]_k - s^k \sum_{i=2}^{k-1} \left(i\, w_i\, f_{k+1-i}\right)$ is the error of order k.

Note that system (82) is a linear system with n equations and $n+1$ unknowns, giving us one degree of freedom. Therefore, we will assume all the terms $f_i = 0\ \forall i > 1$, which is known as a normal form style of parameterization (see [42] for details), resulting in the system:

$$\left[\left(DF(z^*) - \lambda k\, Id\right) w_k\right] s^k = -E_k(s) = -\left[F(W_{<k}(s))\right]_k. \tag{83}$$

Thus, to obtain successive orders of the invariant manifold, we will simply compute the error of order k using automatic differentiation [43], and then solve the linear system (83).

Appendix C. Singularities of the separatrices of the amended pendulum

Consider the Hamiltonian of the amended pendulum

$$P(x, y, \varepsilon) = \frac{y^2}{2} - \frac{2}{3}\varepsilon^2 y^3 + \cos x - 1 \tag{84}$$

and consider the separatrices of the hyperbolic equilibrium point $(0,0)$ defined by $P(x,y,\varepsilon) = 0$. We know that when $\varepsilon = 0$, the separatrices coincide and become singular at $t = \pm \mathrm{i}\pi/2$. So we expect, by continuity, that the singularities of the separatrices $P(x,y,\varepsilon) = 0$ of the amended pendulum are close to them. We will focus on the separatrix such that at $t = 0$ it passes through the point $(x,y) = (\pi, y_0(\varepsilon))$ (when $\varepsilon = 0$, $y_0 = 2$).

So, let us consider the change of time $t = -\mathrm{i}s$ (we will see below that the singularity takes place for $t^* = \mathrm{i}(-s^*)$ with $-s^* = \pi/2 + \delta(\varepsilon) + \mathrm{i}\eta(\varepsilon)$), then the system of ODE associated with (84)

$$\frac{\mathrm{d}x}{\mathrm{d}t} = y - 2\varepsilon^2 y^2,$$
$$\frac{\mathrm{d}y}{\mathrm{d}t} = \sin x,$$

becomes, after the change of variables $x = \mathrm{i}X$, $y = Y$,

$$\frac{\mathrm{d}X}{\mathrm{d}s} = -(Y - 2\varepsilon^2 Y^2),$$
$$\frac{\mathrm{d}Y}{\mathrm{d}s} = \sinh X,$$

which is a Hamiltonian system with Hamiltonian

$$Q(X, Y, \varepsilon) = -\mathrm{i}\, P(\mathrm{i}X, Y, \varepsilon) = -\frac{Y^2}{2} + \frac{2}{3}\varepsilon^2 Y^3 - \cosh X + 1.$$

The following properties can be easily obtained:

$$(P1) \qquad P(\pi, y, \varepsilon) = \frac{y^2}{2} - \frac{2}{3}\varepsilon^2 y^3 - 2,$$

$$(P2) \qquad \cos x = 1 - \frac{y^2}{2} + \frac{2}{3}\varepsilon^2 y^3,$$

$$(P3) \qquad \sin^2 x = \left(\frac{2}{3}\varepsilon^2 y - \frac{1}{2}\right) P(\pi, y, \varepsilon)\, y^2$$
$$= -\frac{2}{3}\varepsilon^2 \left(\frac{2}{3}\varepsilon^2 y - \frac{1}{2}\right)\left(y - y_0(\varepsilon)\right)\left(y - y_1(\varepsilon)\right)\left(y - y_2(\varepsilon)\right) y^2,$$

$$(P4) \qquad y(-\mathrm{i}s) = Y(s)$$

$$(P5) \qquad \sinh X(s) = -\mathrm{i} \sin x(-\mathrm{i}s)$$

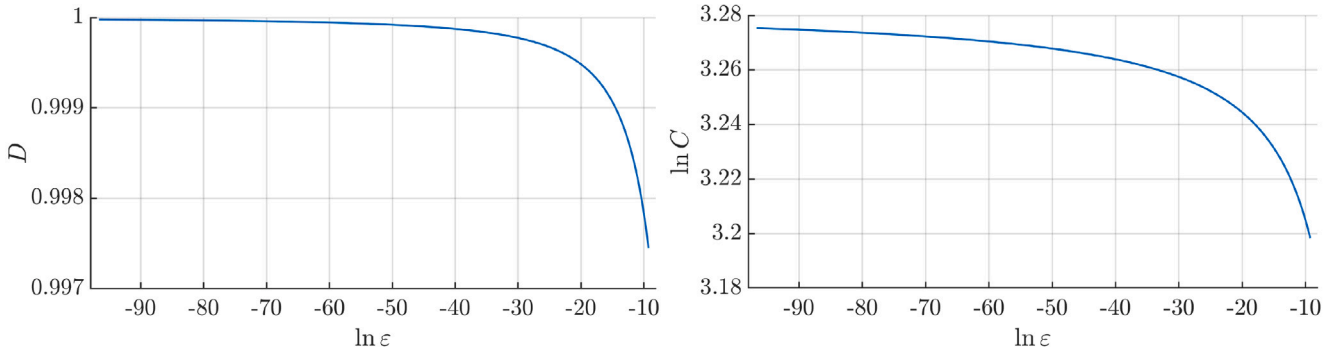

Fig. 17. Values of D (left) and $\ln C$ (right) obtained for the linear fit $\ln \delta(\varepsilon) = D \ln(\varepsilon^2 |\ln \varepsilon|) + \ln C$.

with

$$y_0(\varepsilon) = \frac{\sqrt{3}}{\cos\left(\frac{\pi - \arccos(4\sqrt{3}\varepsilon^2)}{3}\right)}, \qquad y_1(\varepsilon) = \frac{\sqrt{3}}{\cos\left(\frac{\pi + \arccos(4\sqrt{3}\varepsilon^2)}{3}\right)},$$
$$y_2(\varepsilon) = -\frac{\sqrt{3}}{\cos\left(\frac{\arccos(4\sqrt{3}\varepsilon^2)}{3}\right)}.$$

So, we obtain

$$\frac{\mathrm{d}Y}{\mathrm{d}s}(s) = \sinh X(s) = -\sqrt{-\left(1/2 - 2\varepsilon^2 Y(s)/3\right)\left(Y(s) - y_0(\varepsilon)\right)\left(2\varepsilon^2 Y(s)/3 - 2\varepsilon^2 y_1(\varepsilon)/3\right)\left(Y(s) - y_2(\varepsilon)\right)Y^2(s)},$$

that is,

$$-s^* = \int_{y_0(\varepsilon)}^{\infty} \frac{\mathrm{d}Y}{\sqrt{-\left(1/2 - 2\varepsilon^2 Y/3\right)\left(Y - y_0(\varepsilon)\right)\left(2\varepsilon^2 Y/3 - 2\varepsilon^2 y_1(\varepsilon)/3\right)\left(Y - y_2(\varepsilon)\right)Y^2}},$$

which is a convergent improper integral. Equivalently, through the change of variable $Y = 2/v$, we also have

$$-s^* = \int_0^{2/y_0(\varepsilon)} \frac{v\,\mathrm{d}v}{\sqrt{-\left(v - 8\varepsilon^2/3\right)\left(v - 2/y_0(\varepsilon)\right)\left(v - 2/y_1(\varepsilon)\right)\left(v - 2/y_2(\varepsilon)\right)}}.$$

For each given value of $\varepsilon > 0$, we have computed using maple, independently, both improper integrals to double check that both values of s^* coincide. From the numerical computations done, we conclude that s^* has real and imaginary parts, that is, $-s^* = -(\mathrm{Re}\, s^* + \mathrm{i}\, \mathrm{Im}\, s^*)$, where $\mathrm{Re}(-s^*) = \pi/2 + \delta(\varepsilon)$ and $\mathrm{Im}\, s^* = O(\varepsilon^2)$.

Notice that $y(t) = y(-\mathrm{i}s) = Y(s)$ can be continued from the real axis along the vertical line $t = \mathrm{Re}\, t^* + \mathrm{i}s$ for $s \in (0, \mathrm{Im}\, t^*)$, so t^* is a *visible* singularity as introduced in [34].

Our next purpose is to have a fit estimate of $\mathrm{Re}(-s^*) = \pi/2 + \delta(\varepsilon)$ when varying ε, or, more precisely, of $\delta(\varepsilon) = \mathrm{Re}(-s^*) - \pi/2$. Taking values of $\varepsilon \in [10^{-42}, 10^{-4}]$ (see Fig. 16) the following fit is obtained

$$\delta(\varepsilon) \sim C\, \varepsilon^2 \ln \varepsilon. \tag{85}$$

This kind of fit expression can be seen, on the one hand, in Fig. 17, which shows the results of the linear fit $\ln \delta(\varepsilon) = D \ln(\varepsilon^2 |\ln \varepsilon|) + \ln C$. On the left, we see the value of D, which tends to 1 as ε decreases. On the right, we observe the value of $\ln C$ (notice that it would be necessary to take a much smaller range of values of ε to numerically compute the value of C). On the other hand, in Fig. 18 the value of D is displayed for the linear fit $\ln \delta(\varepsilon) = D_j \ln(\varepsilon^2 |\ln \varepsilon|^j) + \ln C_j$, with $j = 0, 1, 2$, which leads us to conjecture the fit expression of $\delta(\varepsilon)$ provided in (85).

So we can infer, taking into account the relations $K = 3\varepsilon^4$, $\omega = -1/(3\varepsilon^2)$, that $\delta(\varepsilon)$ in terms of K is of order $\sqrt{K} \ln K$, or in terms of ω is of order $\frac{1}{|\omega|} \ln \frac{1}{|\omega|}$. We finally remark that the expression for the fit of $\delta(\varepsilon)$ being of the form $C\varepsilon^2 \ln \varepsilon$ instead of $C\varepsilon^2$ (which is the usual situation in papers focussed on this kind of analysis) stimulates future theoretical analysis.

Data availability

Data will be made available on request.

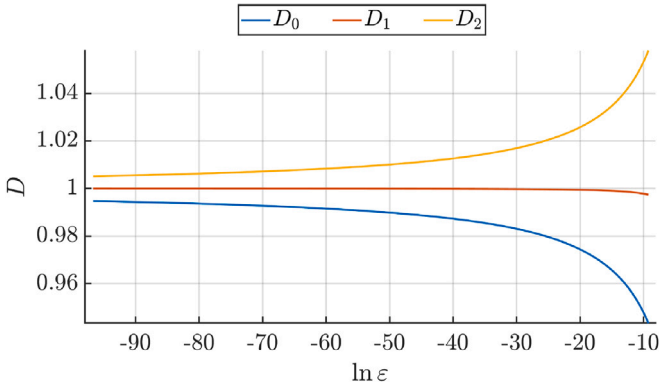

Fig. 18. Values of D_j for the linear fits $\ln \delta(\epsilon) = D_j \ln(\epsilon^2 |\ln \epsilon|^j) + \ln C_j$ for $j = 0, 1, 2$.

References

[1] P. Fu, T.J. Scholz, J.M. Hettema, T.F. Gallagher, Ionization of rydberg atoms by a circularly polarized microwave field, Phys. Rev. Lett. 64 (1990) 511–514.
[2] S. Undurti, H. Xu, X. Wang, A. Noor, W. Wallace, N. Douguet, A. Bray, I. Ivanov, K. Bartschat, A. Kheifets, R. Sang, I. Litvinyuk, Attosecond angular streaking and tunnelling time in atomic hydrogen, Nature 568 (2019) 75–77.
[3] J.H. Bauer, F. Mota-Furtado, P.F. O'Mahony, B. Piraux, K. Warda, Ionization and excitation of the excited hydrogen atom in strong circularly polarized laser fields, Phys. Rev. A 90 (2014) 063402.
[4] K. Rzążewski, B. Piraux, Circular rydberg orbits in circularly polarized microwave radiation, Phys. Rev. A 47 (1993) R1612–R1615.
[5] M.J. Raković, S. Chu, Approximate dynamical symmetry of hydrogen atoms in circularly polarized microwave fields, Phys. Rev. A 50 (1994) 5077–5080.
[6] K. Ganesan, R. GiBarowski, Chaos in the hydrogen atom interacting with external fields, Pramana J. Phys. 48 (2) (1997) 379–410.
[7] C. Jaffé, D. Farrelly, T. Uzer, Transition state theory without Time-Reversal symmetry: Chaotic ionization of the hydrogen atom, Phys. Rev. Lett. 84 (2000) 610–613.
[8] M. Ollé, J.R. Pacha, Hopf bifurcation for the hydrogen atom in a circularly polarized microwave field, Comm. Nonlinear Sci. Numer. Simul. 62 (2018) 27–60.
[9] J. Zakrzewski, D. Delande, J.C. Gay, K. Rzazewski, Ionization of highly excited hydrogen atoms by a circularly polarized microwave field, Phys. Rev. A At. Mol. Opt. Phys. 47 (4A) (1993) R2468–R2471.
[10] I. Bialynicki-Birula, M. Kalinski, J. Eberly, Lagrange equilibrium points in celestial mechanics and nonspreading wave packets for strongly driven rydberg electrons, Phys. Rev. Lett. 73 (13) (1994) 1777–1780.
[11] J.A. Griffiths, D. Farrelly, Ionization of Rydberg atoms by circularly and elliptically polarized microwave fields, Phys. Rev. A 45 (1992) R2678–R2681.
[12] A. Buchleitner, D. Dominique, J.C. Gay, Microwave ionization of three-dimensional hydrogen atoms in a realistic numerical experiment, J. Opt. Soc. Am. B Opt. Phys. 12 (4) (1995) 505–519.
[13] R. Geƀarowski, J. Zakrzewski, Ionization of hydrogen atoms by circularly polarized microwaves, Phys. Rev. A 51 (1995) 1508–1519.
[14] D. Farrelly, T. Uzer, Ionization mechanism of rydberg atoms in a circularly polarized microwave field, Phys. Rev. Lett. 74 (1995) 1720–1723.
[15] A. Brunello, T. Uzer, D. Farrelly, Hydrogen atom in circularly polarized microwaves: Chaotic ionization via core scattering, Phys. Rev. A 55 (5) (1997) 3730–3745.
[16] E. Barrabés, M. Ollé, F. Borondo, D. Farrelly, J. Mondelo, Phase space structure of the hydrogen atom in a circularly polarized microwave field, Phys. D 241 (4) (2012) 333–349.
[17] M. Ollé, To and fro motion for the hydrogen atom in a circularly polarized microwave field, Comm. Nonlinear Sci. Numer. Simul. 54 (2018) 286–301.
[18] E. Barrabés, M. Ollé, Ó. Rodríguez, On the collision dynamics in a molecular model, Phys. D 460 (2024) 1–31.
[19] V.I. Arnold, V.V. Kozlov, A.I. Neishtadt, Mathematical Aspects of Classical and Celestial Mechanics, third ed., in: Encyclopaedia of Mathematical Sciences, Vol. 3, Springer-Verlag, Berlin, 2006, p. xiv+518, [Dynamical systems. III], Translated from the Russian original by E. Khukhro.
[20] À. Jorba, M. Zou, A software package for the numerical integration of ODEs by means of high-order Taylor methods, Experiment. Math. 14 (1) (2005) 99–117.
[21] L. Fousse, G. Hanrot, V. Lefèvre, P. Pélissier, P. Zimmermann, MPFR: A multiple-precision binary floating-point library with correct rounding, ACM Trans. Math. Software 33 (2) (2007) 13–es.
[22] I. Baldomá, M. Giralt, M. Guardia, Breakdown of homoclinic orbits to L_3 in the RPC3BP (I). Complex singularities and the inner equation, Adv. Math. 408 (6) (2022).
[23] I. Baldomá, M. Giralt, M. Guardia, Breakdown of homoclinic orbits to L_3 in the RPC3BP (II). An asymptotic formula, Adv. Math. 430 (109218) (2023).
[24] C. Simó, Averaging under fast quasiperiodic forcing, in: Hamiltonian Mechanics (ToruŃ, 1993), in: NATO Adv. Sci. Inst. Ser. B: Phys., Vol. 331, Plenum, New York, 1994, pp. 13–34.
[25] M. Guardia, C. Olivé, T.M. Seara, Exponentially small splitting for the pendulum: a classical problem revisited, J. Nonlinear Sci. 20 (5) (2010) 595–685.
[26] I. Baldomá, P. Martín, The inner equation for generalized standard maps, SIAM J. Appl. Dyn. Syst. 11 (3) (2012) 1062–1097.
[27] M. Guardia, Splitting of separatrices in the resonances of nearly integrable Hamiltonian systems of one and a half degrees of freedom, Discrete Contin. Dyn. Syst. 33 (7) (2013) 2829–2859.
[28] A. Delshams, T.M. Seara, Splitting of separatrices in Hamiltonian systems with one and a half degrees of freedom, Math. Phys. Electron. J. 3 (1997) Paper 4, 40.
[29] I. Baldomá, The inner equation for one and a half degrees of freedom rapidly forced Hamiltonian systems, Nonlinearity 19 (6) (2006) 1415–1445.
[30] I. Baldomá, E. Fontich, M. Guardia, T.M. Seara, Exponentially small splitting of separatrices beyond Melnikov analysis: rigorous results, J. Differential Equations 253 (12) (2012) 3304–3439.
[31] M. Guardia, P. Martín, T.M. Seara, Oscillatory motions for the restricted planar circular three body problem, Invent. Math. 203 (2) (2016) 417–492.
[32] I. Baldomá, E. Fontich, P. Martín, Invariant manifolds of degenerate tori and double parabolic orbits to infinity in the $n+2$-body problem, Arch. Ration. Mech. Anal. 248 (3) (2024) 94.
[33] K. Meyer, G. Hall, Introduction to Hamiltonian Dynamical Systems and the N-Body Problem, Applied Mathematical Sciences, Vol. 90, Springer-Verlag, New York, 1992, p. xii+292.
[34] V. Gelfreich, C. Simó, High-precision computations of divergent asymptotic series and homoclinic phenomena, Discrete Contin. Dyn. Syst. Ser. B 10 (2–3) (2008) 511–536.
[35] A. Delshams, P. Gutiérrez, Splitting potential and the Poincaré-Melnikov method for whiskered tori in Hamiltonian systems, J. Nonlinear Sci. 10 (4) (2000) 433–476.
[36] O. Koltsova, L. Lerman, A. Delshams, P. Gutiérrez, Homoclinic orbits to invariant tori near a homoclinic orbit to center-center-saddle equilibrium, Phys. D 201 (3–4) (2005) 268–290.
[37] J. Guckenheimer, P. Holmes, Nonlinear Oscillations, Dynamical Systems and Bifurcations of Vector Fields, Springer-Verlag, 1983.
[38] D.V. Treschev, Splitting of separatrices for a pendulum with rapidly oscillating suspension point, Russ. J. Math. Phys. 5 (1) (1997).
[39] X. Cabré, E. Fontich, R. de la Llave, The parameterization method for invariant manifolds I: Manifolds associated to non-resonant subspaces, Indiana Univ. Math. J. 52 (2003).
[40] X. Cabré, E. Fontich, R. de la Llave, The parameterization method for invariant manifolds II: regularity with respect to parameters, Indiana Univ. Math. J. 52 (2003).
[41] X. Cabré, E. Fontich, R. de la Llave, The parameterization method for invariant manifolds III: overview and applications, J. Differential Equations 218 (2005).
[42] À. Haro, M. Canadell, J. Figueras, A. Luque, J. Mondelo, The Parameterization Method for Invariant Manifolds: From Rigorous Results to Effective Computations, first ed., in: Applied Mathematical Sciences 195, Springer International Publishing, 2016.
[43] A. Griewank, A. Walther, Evaluating Derivatives, second ed., Society for Industrial and Applied Mathematics, 2008.